DGFI Report
No. 81

EOT08a – empirical ocean tide model from multi-mission satellite altimetry

Roman Savcenko and Wolfgang Bosch

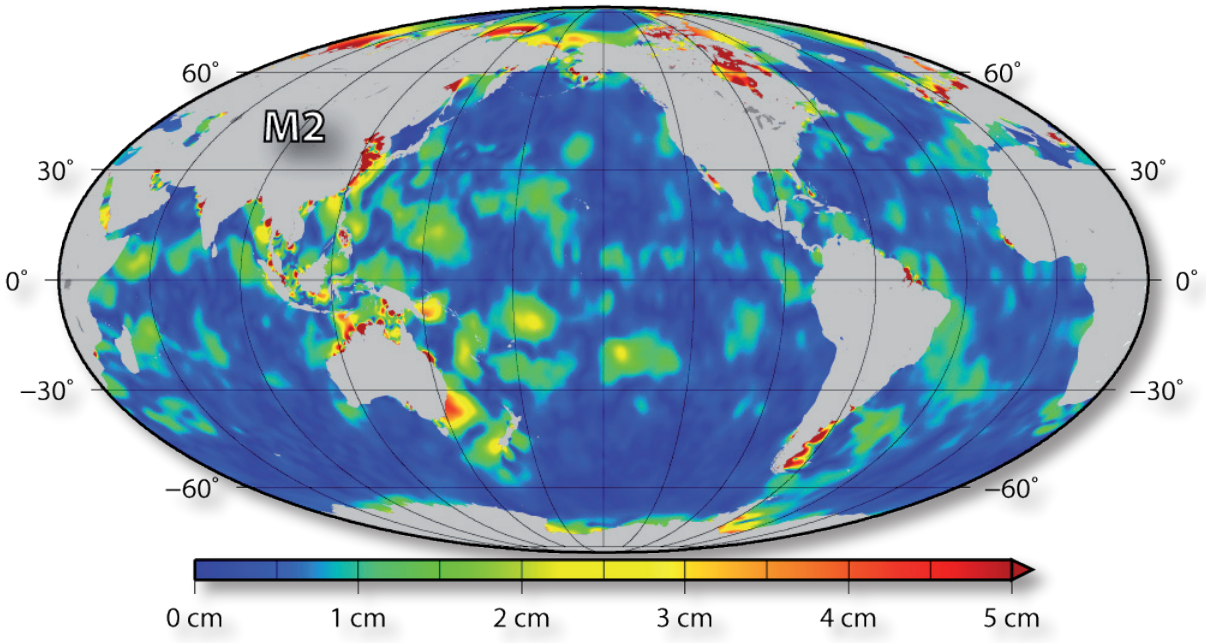

Deutsches Geodätisches Forschungsinstitut (DGFI)
Alfons-Goppel-Str. 11, D-80539 München. Germany
2008

Deutsches Geodätisches Forschungsinstitut
Alfons-Goppel-Straße 11
D-80539 München

Tel. +49 89 23031-1115
Fax: +49 89 23031-1240

email: mailer@dgfi.badw.de

http://www.dgfi.badw.de

Table of Contents

Abstract

EOT08a is a new global solution for the amplitudes and phases of the most dominant ocean tide constituents based on an empirical analysis of multi-mission satellite altimetry data. EOT08a benefits from FES2004, a hydrodynamic model widely used for altimetry and taken as reference model in GRACE gravity field modeling. In shallow water areas the M2 and S2 constituents show numerous extended patterns with residuals taking amplitudes of up to 15 cm. Other major constituents and the non-linear shallow water tide M4 hit residual amplitudes up to 5 cm. Validation at altimeter crossovers and with independent bottom pressure data confirm the significance of these findings. A correlation analysis proves the separability of the analyzed constituents.

1 Introduction

The knowledge of ocean tides is of fundamental importance as the gravitational attraction of Sun and Moon causes more than 80% of the total variability of sea surface (Le Provost 2001). Prediction of ocean tides is crucial for the coastal environment and the protection of its ecosystem, the livelihood of many millions of people. But knowledge of ocean tides is also needed for the precise treatment of space observations. Global ocean tide models quantify loading effects for stations on land, and explain part of the variation observed in Earth rotation Altimetric sea surface heights are to be de-tided in order to be comparable with each other, to allow assimilation into numerical models, and to estimate the mean sea surface. Also, the precise modeling of the Earth gravity field requires reducing not only the direct potential of Sun and Moon, but also the gravitational potential caused by the tidal re-distribution of water masses. The latter is of particular concern in the analysis of data of the GRACE mission. As the ocean tides (with periods of about 12 and 24 hours) are only rarely sampled by GRACE, the tidal signal (and their errors) can be recognized only after rather long "alias" periods. The uncertainties in the tide model are supposed as a possible reason for the meridional stripes which are still present in all satellite-only gravity field solutions obtained from GRACE data. This is the basic motivation of the investigations presented here. This report compiles results obtained in the context of DAROTA, a project of the priority program "Mass transport and mass distribution in the Earth system", funded by the Deutsche Forschungsgemeinschaft (DFG).

2 State-of-the-art of global ocean tide models

Substantial progress in modeling of ocean tides has been achieved through the analysis of increasingly long time series of satellite altimetry data and refinements in hydrodynamic modeling. This progress is indicated by a considerable number of improved ocean tide models, e.g. GOT99.2b and GOT00.2 (Ray 1999), NAO99 (Matsumoto et al. 2000), CSR4.0 (Eanes 1999), FES2002 (Le Provost et al. 1998), FES2004 (Lettellier et al. 2004, Lyard 2006), TPXO6.2 (Egbert & Erofeeva 2002). TPXO7.1 (Egbert, 2007) and GOT4.7 (Ray, 2008) are the latest revisions of the TPXO and GOT model series.

In general ocean tides are known in deep ocean to within 2cm rms at wavelengths of 50 km (Shum et al. 2001). However, tides are significant less known in coastal regions, over continental shelves and in polar oceans. Current investigations show that all state-of-the-art ocean tide models

- have significant errors for S2 and M2 e.g. in Antarctica (Wünsch et al., 2005, King and Padman, 2005) which are due to poor or missing altimetry and tide data at high latitudes,
- have alias frequencies (with GRACE) much longer than 30 days for S2 and K2 leaving the errors of these constituents almost unreduced in monthly gravity field solutions (Knudsen, 2002), (Mayer-Gürr, 2005, unpublished), and
- are still not able to predict the water level in shallow water with sufficient precision (Savcenko & Bosch, 2004)

There are clear indications, however, that these problems can be remedied: Han and Shum (2005) already demonstrated that it is possible to solve for S2

and M2 tides with a spatial resolution as short as 300 km from GRACE data only. Anderson (1999) and Smith et al. (2000) have shown that it is possible to improve the ocean tide models in shallow water and to estimate also non-linear terms like M4. The TOPEX altimeter mission observed for more than 10 years over the same ground track hereby allowing resolving and separating all dominant tidal constituents. Since February 2002 Jason1 continues observation over the same ground track while a few months later the TOPEX orbit was shifted in order to double the spatial resolution. Tide analysis with altimeter data from both ground track systems are now capable to provide significant improvements for the dominant tidal constituents and non-linear shallow water effect like M4 and M6.

The GRACE Science Data System processing centres at CSR, GFZ, and JPL agreed to use FES2004 for de-aliasing of the release 04 GRACE gravity field solutions. This was because FES2004 has been shown to perform better than other recent models like CSR4.0 or GOT00. FES2004 has been also used for altimetry data. In fact to harmonize the multi-mission data base maintained at DGFI the ocean tide corrections of all altimeter systems have been computed with the FES2004 model (the improved release with K2 taken from FES2002 and S1 replaced). This is the reason why in this study FES2004 is taken as a reference and a tidal analysis is performed for the residuals only.

3 Residual tide analysis of altimeter data

Two methods can be used for the empirical estimates of tides, least squares harmonic analysis and the so called response method - each one with its own pros and cons. While the response method (Cartwright and Ray, 1990, Desai and Wahr, 1995, and Smith, 1999) aims to determine the whole diurnal and semidiurnal spectra, the harmonic analysis estimates amplitudes and phases of particular tidal constituents with predefined periods (Schrama and Ray, 1994 and Ray, 1999). The response method is more appropriate for estimating weak tides. However, it is not applicable for the global estimation of non-linear tides: the assumption of a smooth admittance function is violated in some parts of the ocean – the admittances can even exhibit strong resonant picks. Compared to precise tide gauge records the signal to noise ratio of altimeter data is too poor for identifying minor tidal constituents. Neglecting minor tides leads – in general – to background noise, however in case of a residual tide analysis this background noise is significantly mitigated: The a priori tide model takes care of minor tides using the admittance theroy. The harmonic analysis is applied here (see section 3.2) because this study focuses on improvements over shallow water where the assumption of a smooth admittance is difficult to justify.

The tide analysis with altimeter data faces two difficulties - the alias effect and the problem of de-correlating tidal signals with alias periods very close to each other. Alias effects emerge if the altimeter systems sample high frequency tide signals with periods of some 12 and 24 hours only every few days (the satellite repeat period). In this case the tides appear as signals with periods much longer than the sampling interval. These periods – called alias periods – are different for the tidal constituents and depend on the repeat period of the altimeter satellite, see tabulated alias periods in Smith (1999) and Andersen (1999). The capability to separate neighbouring periods from each other is expressed by the Rayleigh criterion. In case of the empirical

tide analysis by altimetry the Rayleigh criterion must be applied to the alias periods. The minimal time span needed for the accurate separation of two tides is called Rayleigh period. For the tidal analysis of altimeter data these periods can again become very large – even infinite if one of the tidal signals cannot be de-aliased at all. A comprehensive discussion on the alias and Rayleigh periods can be found in Smith (1999).

With some thirteen years the altimeter time series on the TOPEX ground tracks (observed by TOPEX and its follow-on, Jason1) is long enough to de-alias all major tidal constituents and also fulfils the Rayleigh criterion for their de-correlation. The time series of 35-day repeat periods of the sun synchronous missions ERS and ENVISAT are, however, problematic in resolving and separating several tidal constituents. The tide constituents S2, K1 and P1 are affected by severe correlation problems and cannot be estimated using the data of these missions alone. The M2 and N2 tides can be separated from each other only if at least a nine years time series of data is available.

The difficulties on alias and Rayleigh periods apply if the data of a single mission at a particular point is considered. Using data on crossing or adjacent tracks already improves the temporal resolution and can in general mitigate the alias effect. The advantage of a complementary sampling on single satellite crossover points depends of the tidal constituent and the latitude (Smith 1999). The most efficient solution to de-alias and de-correlate the constituents is achieved by combining time series of missions with different sampling characteristics. This combination requires a careful preprocessing of altimeter data which is briefly described in the following section.

3.1 Altimeter data pre-processing

The tidal analysis was based on the common use of altimeter data of TOPEX, Jason-1, ERS-1, ERS-2, ENVISAT, and GFO, acquired during the 13 years life time of TOPEX (c.f. Table 1). Combining altimeter data of different missions requires three pre-processing steps: upgrading, harmonization and cross-calibration.

Upgrading means to use the most recent (re-tracked) observation data, mission specific correction models, and orbital ephemeredes. For the ESA missions new orbits were taken from Scharroo & Visser, (1998). All ERS-1 and ERS-2 specific corrections recommended by Schrama et al. (2000) have been applied. The wet tropospheric correction for ERS-2 were computed using the algorithm described in Eymard et al. (2003). The orbits of ENVISAT were replaced by GRACE-based orbits from DEOS. For TOPEX, the sea state bias model described by Chambers (2003) was used and the wet tropospheric correction were taken from the JPL "microwave replacement product", version 1.0. (Desai, pers. communication)

Harmonization implies to use as far as possible the same models for geophysical corrections to avoid that model differences are wrongly interpreted as apparent sea level variations. Therefore, for all missions the inverted barometer correction was replaced by the dynamic atmospheric corrections (DAC) produced by CLS Space Oceanography Division using the MOG2D model from LEGOS (Carrère and Lyard, 2003). As already indicated, the ocean tide corrections for all missions were based on the FES2004 (Lyard et al., 2006). All time series analysis are performed with sea level anomalies,

Table 1. Altimeter data used in this study

Mission/Phase	Cycles	Period	Source
TOPEX/Poseidon	001-481	1992/09/23-2005/10/08	MGDR-B (NASA)
Jason-1	001-135	2002/01/15-2005/09/14	GDR-B (CNES/NASA)
ERS-1 (C&G)	083-101	1992/04/14-1993/12/20	OPR-V6 CERSAT
	144-155	1995/03/24-1996/04/28	
ERS-1(D,E&F)	102-143	1993/12/25-1995/03/21	OPR-V3 CERSAT
ERS-2	000-085	1995/04/29-2003/07/02	OPR-V6 CERSAT
ENVISAT	009-040	2002/09/24-2005/09/19	GDR ESA/CNES
GFO	037-159	2000/01/07-2005/10/04	GDR NOAA

deviation of the instantaneous sea level from a mean sea surface. For all altimeter mission the CLS01 mean sea surface (Hernandez & Schaeffer, 2000) was taken as a reference for sea level anomalies.

Finally, a cross calibration was performed by a global crossover analysis based on nearly simultaneous single- and dual satellite crossover differences performed between all altimeter systems operating contemporaneously. This crossover analysis captures not only relative range biases, but also systematic inconsistencies in the center-of-origin realization and geographically correlated errors. Through this cross calibration the radial errors of all satellites was estimated for the complete TOPEX lifetime. Details of this multi-mission cross calibration are described in Bosch (2006). After correcting the radial errors, the data of all missions could be considered as consistent and was subsequently used by the harmonic analysis.

3.2 Harmonic Analysis

The harmonic analysis was applied for the constituents M2, S2, N2, K2, K1, O1, Q1, P1, 2N2 and M4. In addition to the sine and cosine coefficient of these constituent, a mean value, a trend, and annual and semi-annual signals were solved for simultaneously. The least squares approach was applied using the following observation equation.

$$\hat{\zeta} + \hat{v} = m + d \cdot \Delta t + \\ + \sum_i f_i \left[h_{1i} \cos(\omega_i \Delta t + u_i) + h_{2i} \sin(\omega_i \Delta t + u_i) \right] + \\ + \sum_j \left[a_{1j} \cos(\Omega_j \Delta t) + a_{2j} \sin(\Omega_j \Delta t) \right] \quad (1)$$

where

ζ	estimated sea level anomaly
v	estimated residual
m	mean value
d	trend
h_{1i}, h_{2i}	cosine and sine coefficients
ω_i, Δt	astronomical arguments
f_i, u_i	nodal corrections to amplitude and phase
Ω_j	angular frequency for annual and semiannual variations
a_{1j}, a_{2j}	cosine and sine coefficients of (semi)annual variations

To mitigate the correlation problem the analysis was performed on the nodes of a regular 15′×15′ geographical grid. For every grid node normal equations were accumulated using all observations inside a spherical cap and applying a Gauss function for weighting inverse proportional to the grid node distance. The selection of the cap radius and the decay of the Gauss function, controlled by the half weight width, are critical: high weights and a large cap size imply a strong smoothing. Low weights and a small cap size can prevent the desired de-correlation of some constituents. The limiting cap size was always set to three times the half weight width. Based on systematic experiments three different sets of weighting parameters were applied. For the open ocean (depth > 200 m) the half weight width was set to a spherical distance of 1.5°. In shallow water a half weight width of 0.5° was used. For high latitudes (> 65° and < -65°) without TOPEX or Jason-1 data the half weight width was set to 2°.

3.3 Results

Some preliminary investigations performed in the North-West European Shelf and the Patagonian Shelf indicated that in shallow water area residuals with 5 - 10 centimetres amplitude can be expected. This was confirmed by the global analysis of multi-mission altimeter data. For all constituents analyzed significant residual amplitudes were found. Even for the weak 2N2 tide residuals of 1 - 2 cm were identified. The Apendix compiles plots with the residuals of all constituents for the Patagonian Shelf (A.1), the North-West European Shelf (A.2) and the Yellow Sea (A.3). The apendix A.4 show the global distribution of the residuals of all constituents.

As an example Figure 1. shows the global distribution of residual amplitudes estimated for the most dominant tide M2. In shallow water the residuals can reach more than 10 cm amplitude (see Appendicies A.1 - A.3). It is, however, remarkable that the distribution of the M2 residuals shows also large scale pattern in the open ocean. Such large scale pattern with a somewhat lower

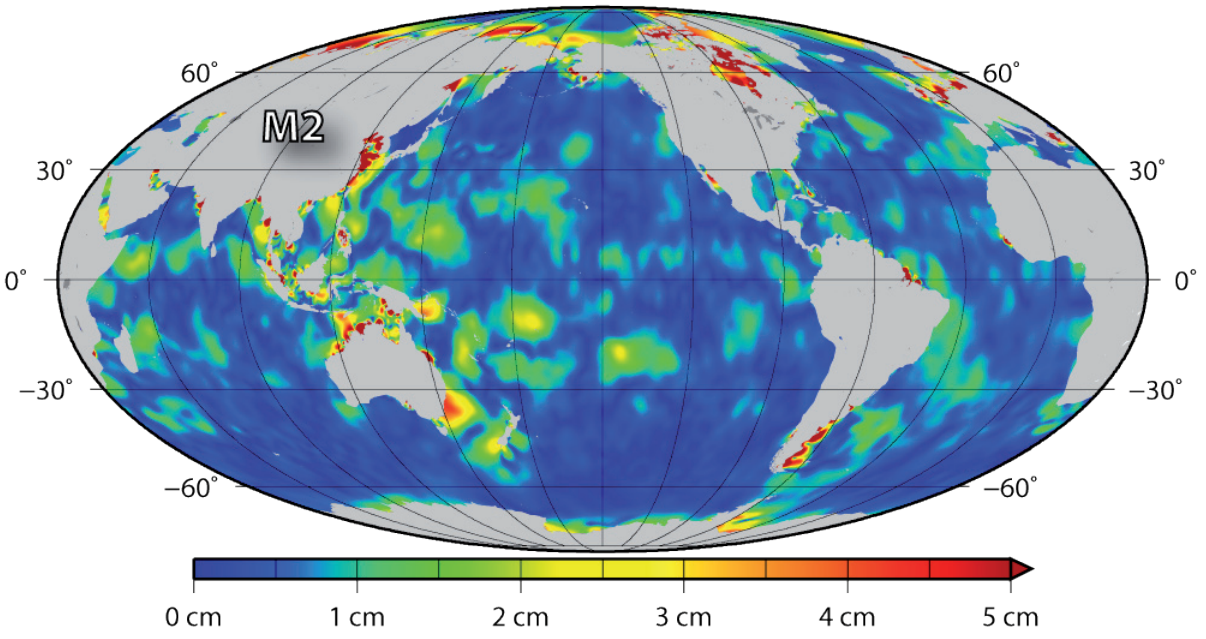

Figure 1 Amplitudes of M2 residuals

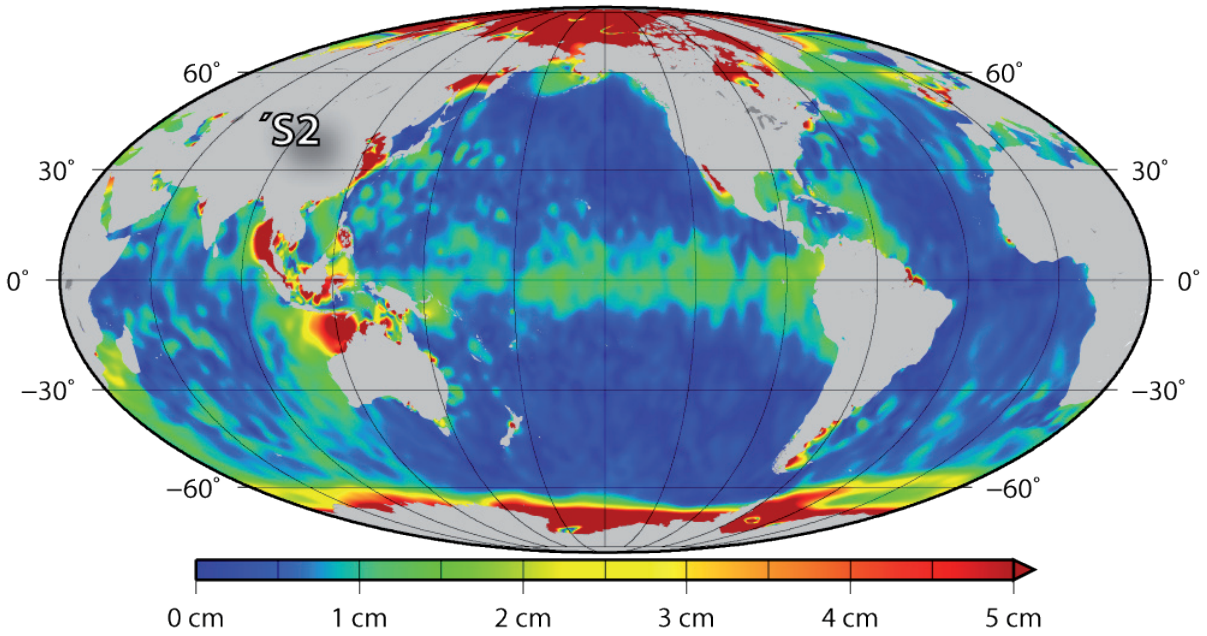

Figure 2 Amplitudes of S2 residuals

amplitude of some 1-2 cm are also present in the results for S2 (see Figure 2) and K2 (see appendix A.4). Figure 2 also shows, that the residuals of S2 are significant larger in polar areas. Obviously, due to the absence of TOPEX and Jason1 data it was not possible to obtain a reliable estimate of S2. Similar problems are seen in the results of P1 and K1.

3.4 Correlation analysis

As multi-mission altimetry is used for this study there is a completly irregular distribution of observations along the ground tracks contributing to each grid node. Consequently there is no simple rule to examine the potential to identify and separate all tidal constituents. It is therefore essential to analyse the correlations among the constituents.

According to Smith (1999) the correlation between two constituents are defined as rms of the correlation between their sine and cosine coefficients.

$$\rho = \sqrt{\frac{1}{4}\left(\rho^2_{C_1C_2} + \rho^2_{C_1S_2} + \rho^2_{S_1C_2} + \rho^2_{S_1S_2}\right)}$$

Similar, the correlation between tides and mean sea level is defined by following formula

$$\rho = \sqrt{\frac{1}{2}\left(\rho^2_{Cm_0} + \rho^2_{Sm_0}\right)}$$

The global mean values of these correlation have been compiled to Table 2. Form most of the constituents the mean correlation remains well below 0.05. Correlations above 0.2 appear only between S2 and the mean value, K2 and the semi-annual variation, Ssa, and between K1 and P1. The latter is caused by the sun-synchronous orbits of ERS and ENVISAT, causing alias periods of about one year for both tides. This implies an infinite Rayleigh period - a separation is only possible by means of satellites with different orbit configuration.

Table 2 Mean correlations between tidal constituents, the shallow water tide M4 and annual and semiannual period

	m0	M2	S2	N2	K2	2N2	O1	K1	P1	Q1	M4	Sa	Ssa
m0	-	0,01	**0,28**	0,01	0,02	0,00	0,01	0,04	0,06	0,01	0,01	0,10	0,05
M2		-	0,01	0,01	0,01	0,01	0,03	0,01	0,01	0,01	0,01	0,01	0,01
S2			-	0.01	0,04	0,01	0,01	0,06	0,05	0,01	0,01	0,04	0,03
N2				-	0,01	0,01	0,01	0,01	0,01	0,03	0,01	0,01	0,01
K2					-	0,01	0,01	0,04	0,07	0,01	0,01	0,02	**0,21**
2N2						-	0,01	0,00	0,00	0,01	0,01	0,01	0,01
O1							-	0,01	0,01	0,01	0,01	0,01	0,01
K1								-	**0,27**	0,01	0,00	0,12	0,07
P1									-	0,01	0,00	0,12	0,04
Q1										-	0,01	0,01	0,01
M4											-	0,00	0,01
Sa												-	0,07
Ssa													-

The geographical distribution of the correlations is shown in Figures 3, 4, and 5.

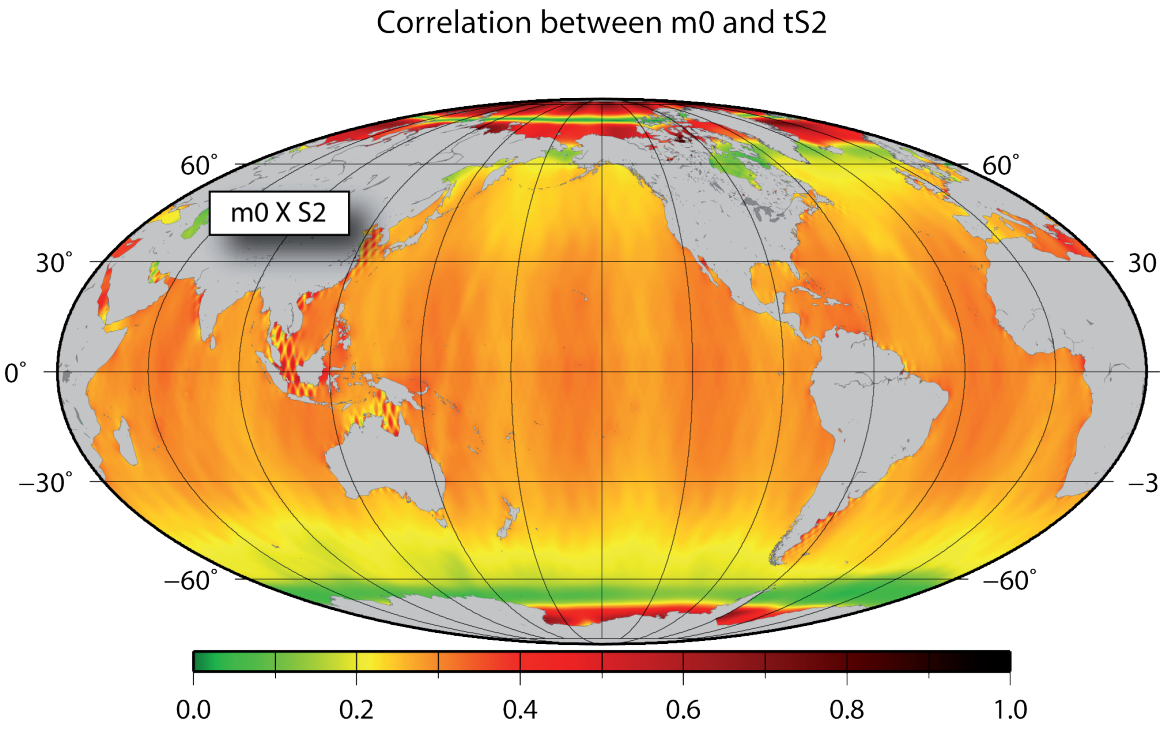

Figure 3 Geographical distribution of the correlation coefficient between m0 and S2

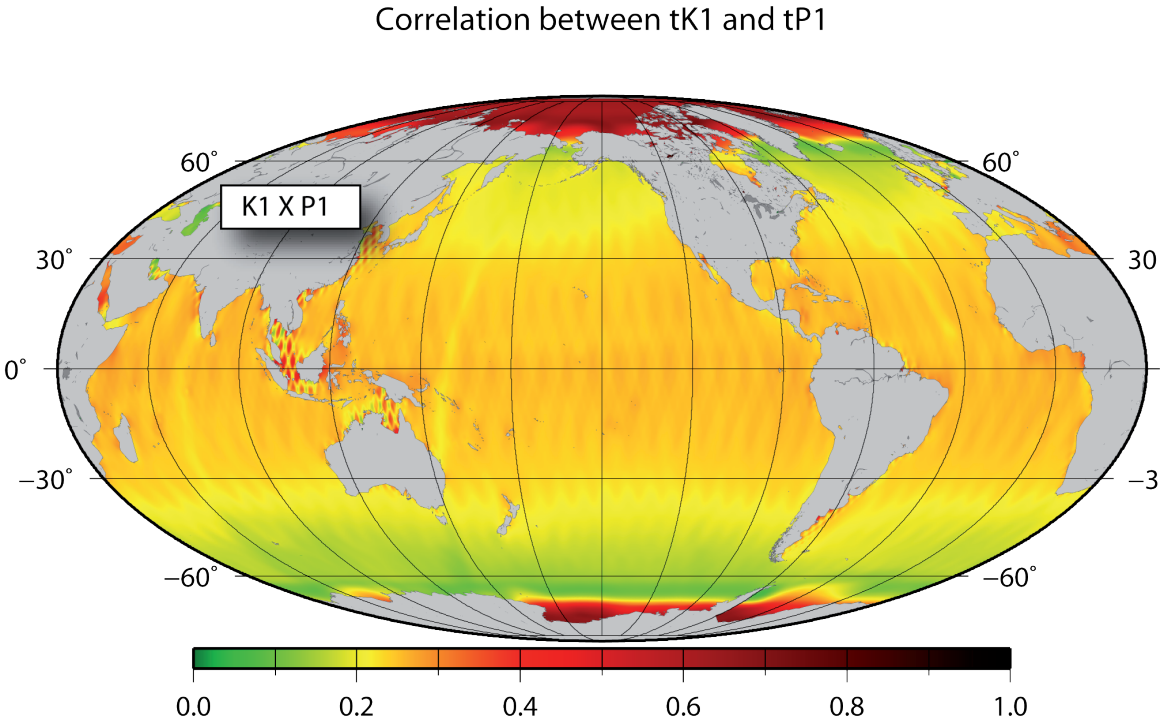

Figure 4 Geographical distribution of the correlation coefficient between K1 and P1

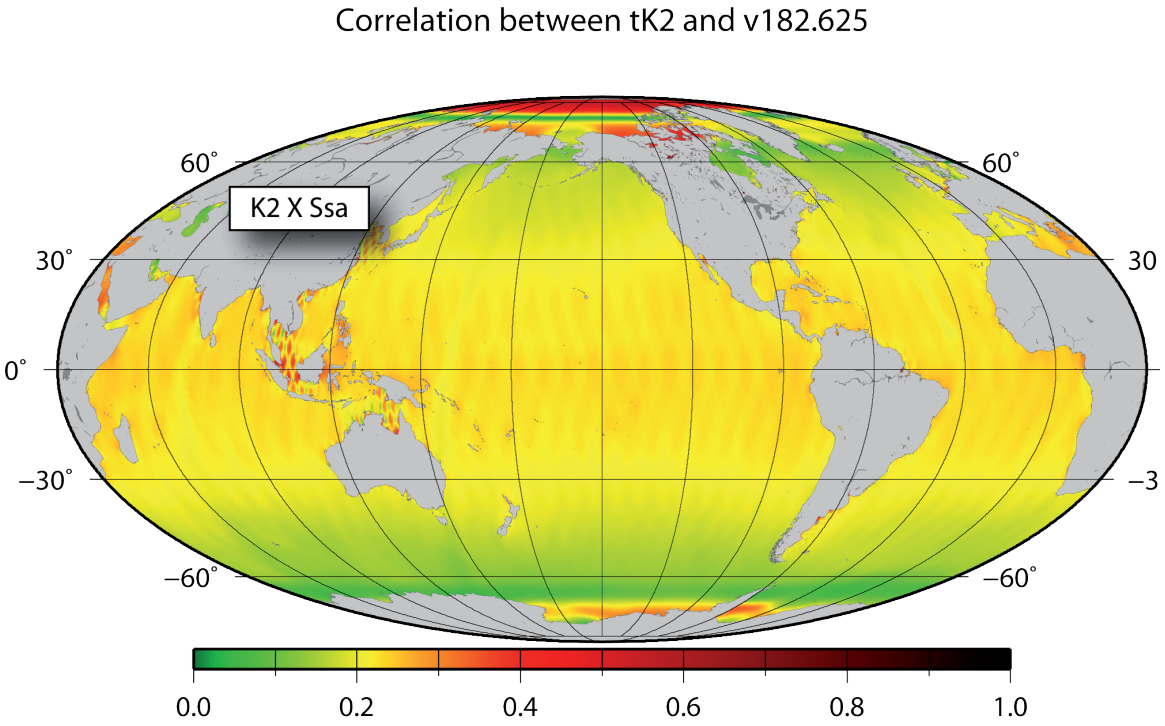

Figure 5. Geographical distribution of the correlation coefficient between K2 ans Ssa.

3.5 Validation of residuals

The residuals estimated by the harmonic analysis can be validated by proving the reduction in variance achieved by applying the residuals to time series containing the ocean tide signal. Such variance reduction tests were carried out at

- a few sites around the British Islands with historical ocean bottom pressure records available from BODC, and
- crossover points of ERS-2, GFO, and TOPEX for the North-West European Shelf and the Yellow Sea.

The first test is more radical, because independent data is used. However, the test is limited as ocean bottom pressure records over other shelves are nearly unavailable (The compilation of such sites is an ongoing activity at DGFI). The test was carried out in two steps. First, the variance σ_{FES} of the time series was computed after correcting for the tidal constituents of FES2004 (see Figure 6, left panel). Second, the estimated residuals were applied in addition and the variance was computed again, now termed as $\sigma_{FES+res}$. The percentage gain

$$100 \cdot (\sigma_{FES+res} - \sigma_{FES}) / \sigma_{FES}$$

is shown in the right panel of Figure 6 and clearly proves the gain achieved by the residual tide analysis. The mean variace reduction is 11%.

The variance reduction test with the altimeter time series of ERS-2, GFO and TOPEX are shown in Figure 7 (for the North-West European Shelf) and in Figure 8 (for the Yellow Sea). It should be emphasized that the complete time series of the missions have been used. All panels identify a clear gain in variance. The mean variance reduction for the North-West European Shelf ist 6%, for the Yellow Sea 26%.

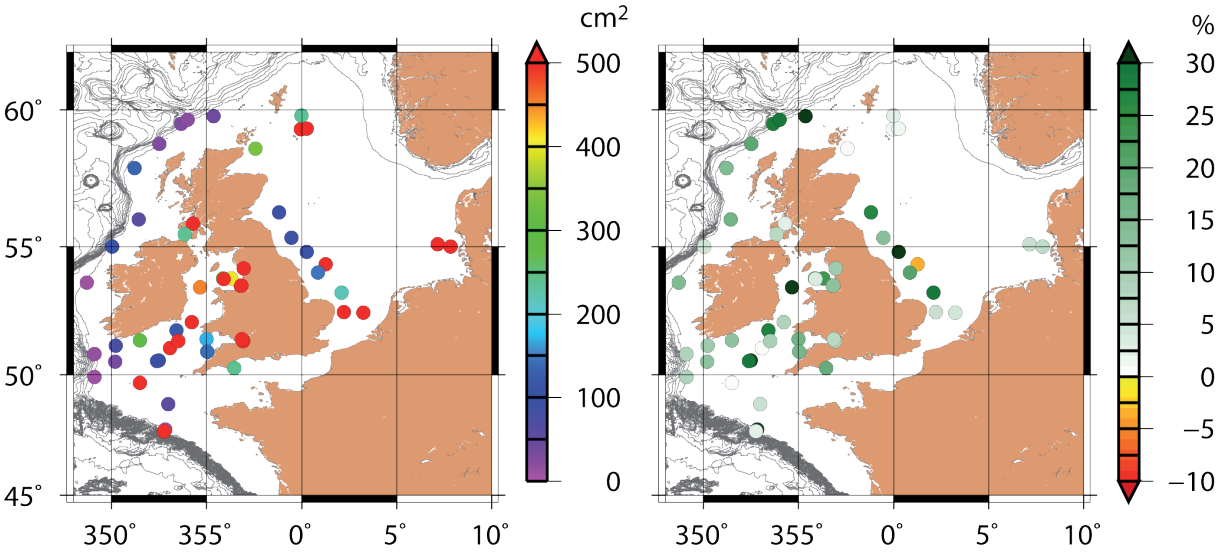

Figure 6 Validation test with ocean bottom pressure records of BODC. Left: variance after correcting the time series for the FES2004 tides. Right: gain in variance achieved after the residuals of this study have been applied in addition.

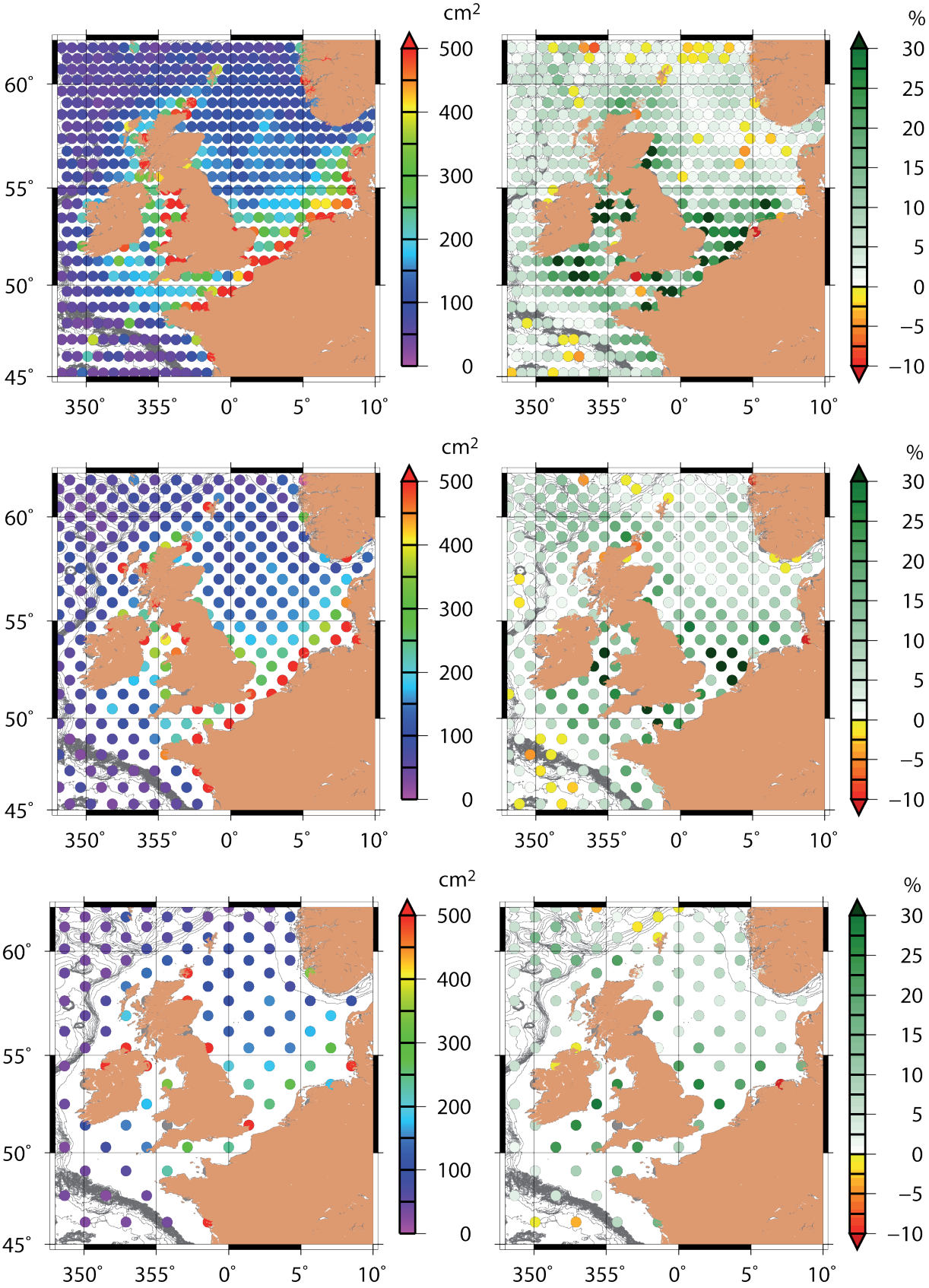

Figure 7 Validation test for the North-West European Shelf with altimeter time series at crossover points of ERS-2 (top row), GFO (middle row), and TOPEX (bootom row). Left: variance after correcting the time series for the FES2004 tides. Right: gain in variance achieved after the residuals of this study have been applied in addition.

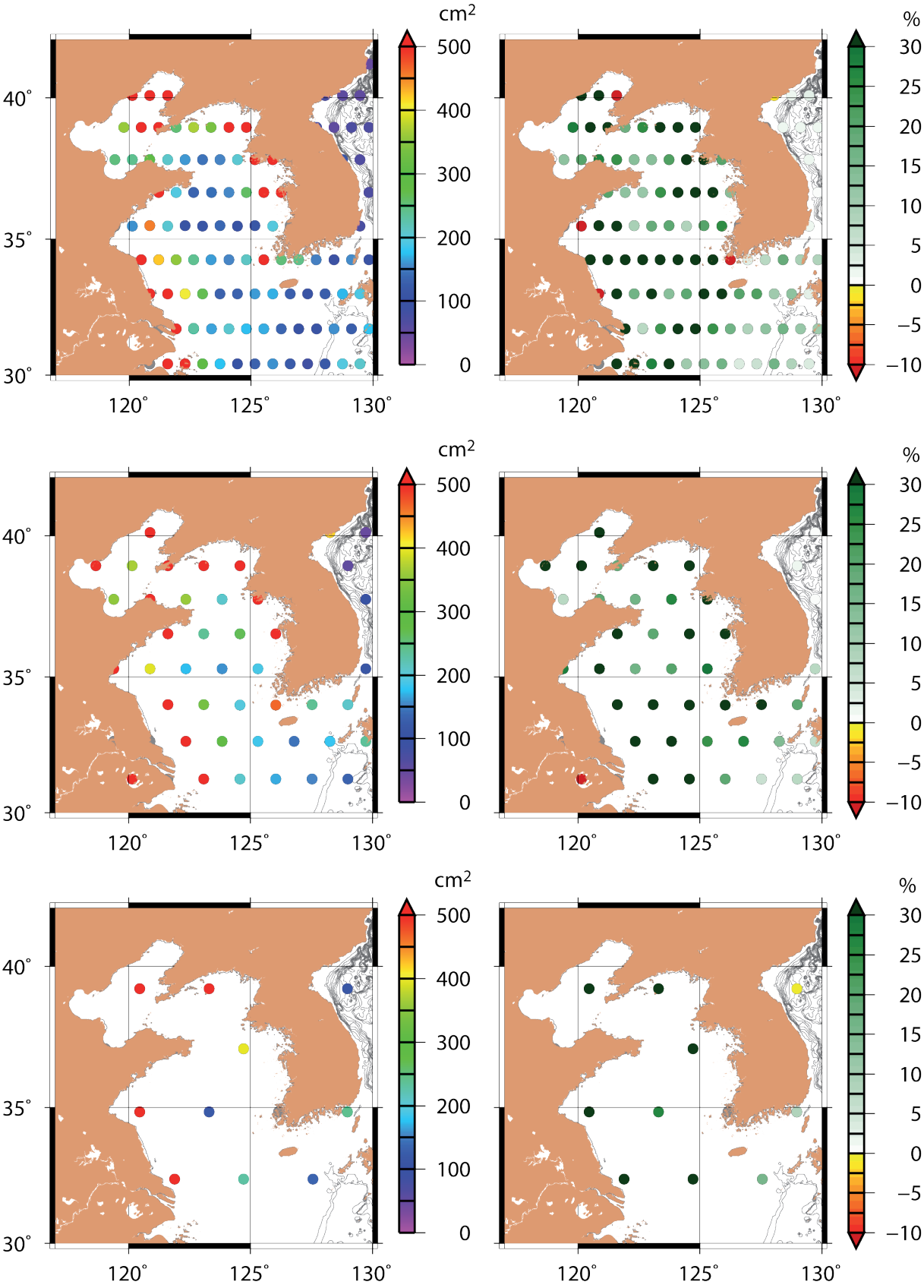

Figure 8 Validation test for the Yellow Sea with altimeter time series at crossover points of ERS-2 (top row), GFO (middle row), and TOPEX (bootom row). Left: variance after correcting the time series for the FES2004 tides. Right: gain in variance achieved after the residuals of this study have been applied in addition.

4 Composing EOT08a

The ocean tide analysis reveals significant residuals and their validation and correlation analysis in general justifies to consider the residuals as definite improvements over the reference model. However, the results are not everywhere of the same reliability. In particular in high latitude areas, where no TOPEX and Jason-1 data are available and where the correlation between critical constituents increases, the confidence into the results is much lower than for the shallow water areas.

Therefore, EOT08a was not composed by simply adding the residuals to the reference model. Instead, following composition strategy for EOT08a was applied:

- Up to latitude ± 67° residual for M2, N2, and M4 were added to the reference model. From ± (67° up to 75°) a transition zone was defined in which these residuals were linear down weighted from 1 to 0. Above ±75° the reference model was not changed at all.
- For the residuals of all other constituents the transition zone was defined by the latitude range ± (62° up to 70°) such that above ±70° EOT08a falls completely back to the reference model.
- Over open ocean the signal-to-noise ratio of the residuals for the (very weak) constituents 2N2 and Q1 were considered to be too poor. Therefore, residuals of 2N2 and Q1 were only used for shallow water areas with a transition zone for depth between 200 and 300 m.

As the analysis was performed for the nodes of a 15'x15' grid and the imporved ocean tide model should be provided with the spatial resolution of the refence model, the composition implied a final interpolation onto the 7.5'x7.5' grid of FES2004.

4.1 Investigating residual loading tides

As the residual tides are very small it can be assumed that the associated loading effects can be neglected. In order to prove this assumption the residual loading tides were computed using the formulae given by Cartwright and Ray (1991) and Ray (1999): If the complex residual tidal admittance is defined by

$$Z(\varphi,\lambda) = \sum_{nm} a_{nm} Y_n^m(\varphi,\lambda)$$

then the complex resdiaul loading admittance is given by

$$Z_{load}(\varphi,\lambda) = \sum_{nm} \beta_n \, a_{nm} Y_n^m(\varphi,\lambda)$$

where

$$\beta_n = \frac{\alpha_n}{1+\alpha_n} \quad \text{and} \quad \alpha_n = \frac{\rho_w}{\rho_e} \cdot \frac{3}{2n+1} \cdot h_n' \ .$$

ρ_w and ρ_e are mean densities of water and solid Earth respectively. The loading coefficients h_n' are taken from Farell (1972). The most dominant constituent M2 was taken and the residuals were developed into spherical har-

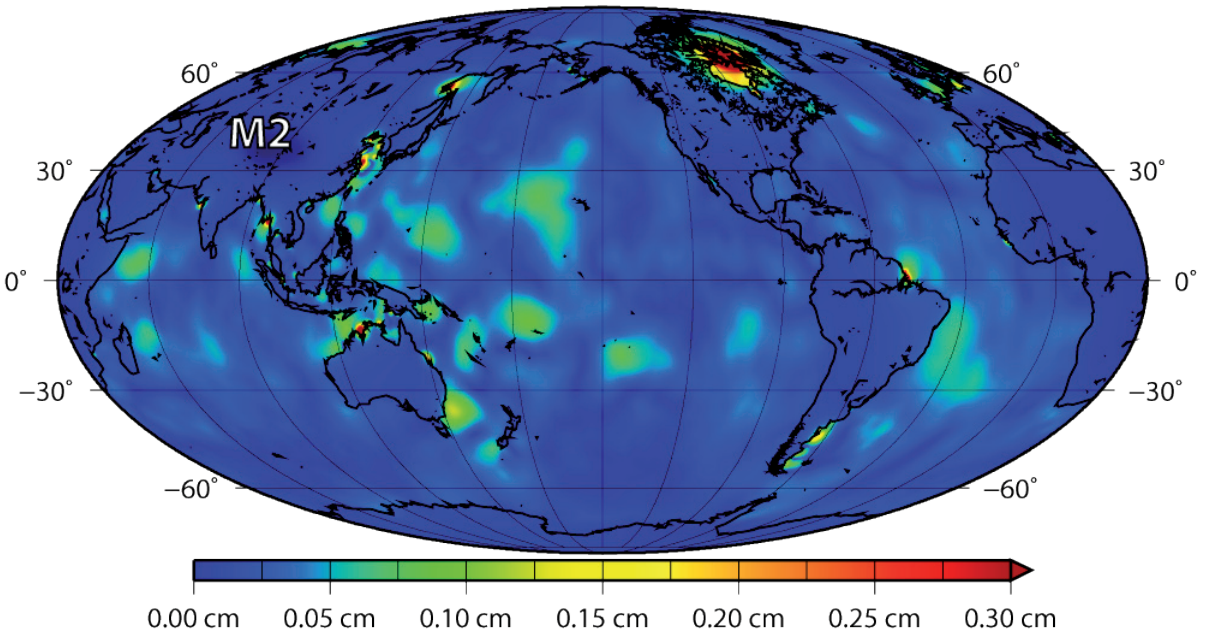

Figure 9. Residual loading effect computed for the M2 resdiuals of this study

monics up to degree and order 720. The residual loading, computed with the formulae above, are shown in Figure 9. As a result, the residual loading effect remains below 2mm such that the loading grids of the refrence model can be taken without change.

4.2 Validation of EOT08a

For the vaildation of EOT08a (and other global ocean tide models) three different data sets are available

1. The (somehow historic) ST102p set of pelagic tides (Ray, pers. comm.) providing tidal constants of 102 sites which are rather regulary distributed over the world ocean but not representative for shallow water (see Figure 10, the red dots)

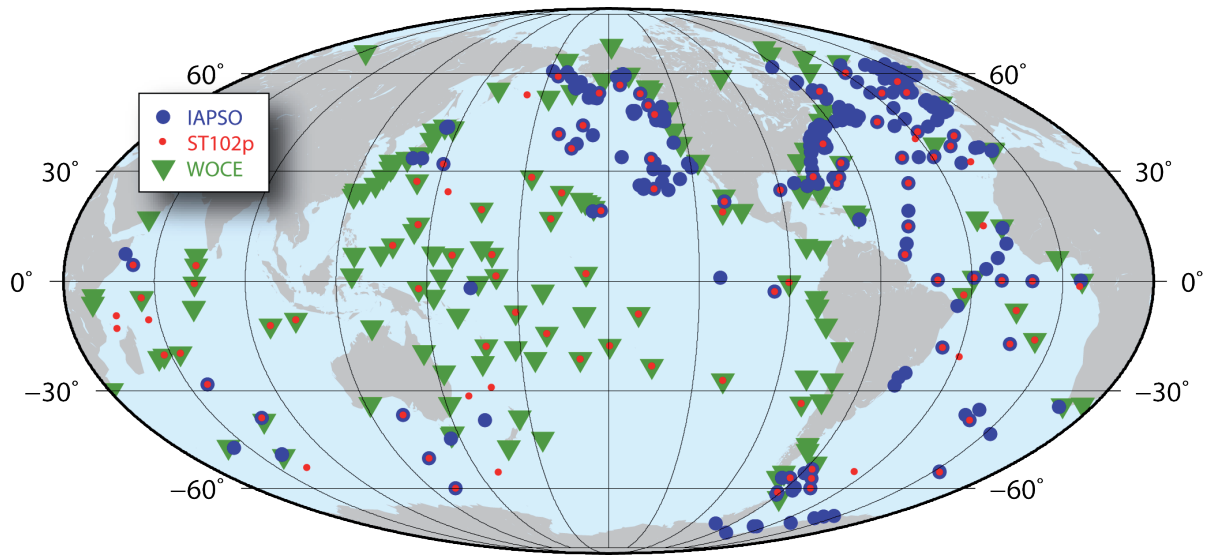

Figure 10. The sites of ST102p (red dots), IAPSO (blue dots) and WOCE (green triangles) with known tidal constants used for EOT08a validation.

2. A set of about 412 sites compiled by IAPSO (Smithson 1992) . These sites are predominantly located in the North Atlantic and the North-East Pacific (see the blue dots in Figure 10). This data set includes a certain number of coastal sites.

3. A compilation of tidal constants for nearly 200 "fast delivery" and "delayed" mode sites of WOCE, provided by the BODC (green triangles in Figure 10). These sites are predominantly coastal tide gauges.

In order to compare the tidal constants of these sites with the global ocean tide models a nearest neighbour interpolation was used and RMS differences were computed for every constituent by means of following formula

$$RMS = \sqrt{\frac{\sum_{i=1}^{n}\left(\left(A_i^{tg}\cos\Phi_i^{tg} - A_i^{m}\cos\Phi_i^{m}\right)^2 + \left(A_i^{tg}\sin\Phi_i^{tg} - A_i^{m}\sin\Phi_i^{m}\right)^2\right)}{2n}}$$

where A_i^{tg} and Φ_i^{tg} are the tidal constants from tide gauges. A_i^{m} and Φ_i^{m} stand for the tidal constants taken from the nearest grid node of the ocean tide model. The RMS values for the models EOT08a, FES2004, GOT4.7 (Ray, 2008) and TPXO7.1 (Egbert) are listed in Table 3.

The RMS comparisons in Table 3 are not very convincing. Compared with FES2004, EOT08a seems to perform slightly better (e.g. for K2, M2 @ ST102p, for K1, K2, M2, P1 @ IAPSO, and for K1, K2, M4, @ WOCE). However, EOT08a has higher RMS differences for S2 @ SST102p. Except for M2 GOT4.7 and TPXO7.1 are performing better than either FES2004 or EOT08a. This is particular true for S2 @ IAPSO.

GOT4.7 is defined on a 30'x30' grid and TPXO7.1 on a 15'x15' grid. The land-ocean mask is not consistent with FES2004 or EOT08a. A consistent extrapolation to coastal sites is difficult and therefore these models were not included in the comparison at the coastal WOCE sites.

Table 3. Statistic of RMS differences between global ocean tide models and the ST102p, IAPSO, and WOCE compilation of tide gauges with known tidal constants

ST102p					
Tide	**EOT08a**	**FES2004**	**GOT4.7**	**TPXO7.1**	**num**
2N2	0.3	0.3	n.a.	n.a.	98
K1	1.1	1.1	1.0	1.0	102
K2	0.4	0.5	0.4	0.4	98
M2	1.5	1.6	1.7	1.5	102
N2	0.7	0.7	0.7	0.6	99
O1	0.8	0.8	0.7	0.8	102
P1	0.4	0.4	0.4	0.4	98
Q1	0.3	0.3	0.3	0.3	96
S2	1.1	0.9	1.0	0.9	102

WOCE			
Tide	**EOT08a**	**FES2004**	**num**
2N2	0.6	0.6	196
K1	4.1	4.3	181
K2	1.6	1.7	179
M2	12.5	12.2	181
M4	1.3	1.5	181
N2	2.7	2.6	181
O1	3.1	3.1	181
P1	1.4	1.4	181
Q1	0.7	0.7	181
S2	4.5	4.5	181

IAPSO					
Tide	**EOT08a**	**FES2004**	**GOT4.7**	**TPXO7.1**	**num**
K1	1.7	1.8	1.4	1.2	412
K2	0.8	0.9	0.7	0.7	372
M2	2.5	2.6	3.0	2.7	412
N2	0.9	0.9	0.9	0.9	406
O1	1.4	1.4	1.0	1.0	411
P1	2.6	2.8	2.6	2.5	372
Q1	0.5	0.5	0.4	0.4	373
S2	1.9	1.9	1.6	1.6	411

5 Conclusions

A thirteen years time series of multi-mission altimeter data has been used to empirically estimate a new global ocean tide model, EOT08a. Harmonic analysis was performed for the nodes of a regular grid. By combining carefully pre-processed altimeter systems with different sampling characteristics the severe alias problems for the time series of ERS, ENVISAT and GFO could be solved. For the most dominant tidal constituents residual tide signals were identified with amplitudes of up to 15 cm in shallow water. Over the open ocean large scale pattern of M2 with 1-2 cm amplitude were found. Validation and correlation analysis justify that the residuals realize significant improvements over the reference model. The small degradation of statistics for S2 tidal constituent will be considered in further studies.

6 References

Andersen,O.B. (1999): Shallow water tides in the northwest European shelf region from TOPEX/ POSEIDONaltimetry. J. Geophys. Res., Vol. 104(C4), 7729-7742, doi: 10.1029/1998JC900112.

Bosch, W. 2006.Satellite Altimetry Cross Calibration. In: P. Tregoning Rizos (Eds): Dynamic Planet Understanding a Dynamic Planet and Oceanographic Tools. IAG 130, 51-56, Springer, Berlin

Carwright D.E. and R.D. Ray(1990): Oceanic Tides From Geosat Altimetry, J. geophys. Res. 92(C3) 3069-2090.

Cartwright D.E. and R.D. Ray(1991): Energetic of Global Ocean Tides From Geosat Altimetry. J. geophys. Res. 96(C9) 16,897-19,912.

Cartwright D.E. and R.D. Ray (1994): On the radiational anomaly in the global ocean tide with reference to satellite altimetry, Oceanologica Acta, 1994, 17,5,453-459

Carrère, L., and F. Lyard (2003), Modeling the barotropic response of the global ocean to atmospheric wind and pressure forcing—comparisons with observations, Geophys. Res. Let., 30(6), 1275, doi: 10.1029/2002GL016473.

Chambers, D. P., S. A. Hayes, J. C. Ries, and T. J. Urban, 2003, New TOPEX sea state bias models and their effect on global mean sea level, J.Geophys. Res., 108(C10), 3305.

Egbert, G.D., and S.Y. Erofeeva (2002): Efficient inverse modelling of barotropic ocean tides, J.Atmos. OceanicTechnol., 19(2), 183-204.

Egbert (2007), TPXO7.1, http://www.esr.org/polar_tide_models/Model_TPXO71.html

Eymard, L, E. Obliges and N. Tran, 2003, ERS2/ MWR drift evaluation and correction, Rep. CLS.DOS/NT/03.688

Farrell, W.E.: Deformation of the Earth by surface loads. Rev. Geophys. Space Phys., 10, 761-797, 1972.

Han, S.C., Shum C.K., and Matsumoto, K. (2005), GRACE observations of M2 and S2 ocean tides underneaththe Filchner-Ronne and Larsen ice shelves, Geophys. Res. Let, 32, L20311, doi: 10.1029/2005GL024296.

Hernandez, F. and P. Schaeffer, 2000, Altimetric Mean Sea Surfaces and GravityAnomaly maps inter- comparisons AVI-NT-011-5242-CLS, 48 pp. CLS Ramonville St Agne.

King and Padman (2005), Accuracy assessment of ocean tide models around Antarctica, Geophys. Res. Let, 32,L23608, doi: 10.1029/2005GL023901.

Knudsen, P. (2002), Correcting GRACE gravity fields for ocean tide effects, Geophys. Res. Let, 29(8), doi:10.1029/2001GL0114005.

Le Provost C., 2001. Ocean Tides. In: Satellite Altimetry and Earth Sciences. Ed. L.L. Fu and A. Cazenave. Academic Press, 2001.

Le Provost, C. (2002), FES2002 – A new version of the FES tidal solution series, Abstract Volume, Jason-1 Science Working Team Meeting, Biarritz, France.

Lettellier T., F. Lyard, and F. Lefebre (2004): The new global tidal solution: FES2004. Presented at: OceanSurface Topography Science Team Meeting, St. Petersburg, Florida, Nov. 4-6.

Lefevre F., F. Lyard, C. Le Provost and E.O. Schrama FES99: A Global Tide Finite Element Solution Assimilating Tide Gauge and Altimetric Information.", JAOT, 2002, Vol. 19, 1345--1356

Lyard F., Lefevre F., Letellier T., and Francis O. (2006), Modelling the global ocean tides: modern insights from FES2004. Ocean Dynamics, 56, 394–415, doi:10.1007/s10236-006-0086-x.

Matsumoto, K., T. Takanezawa, and M. Ooe (2000): Ocean tide models developed by assimilatingTOPEX/POSEIDON altimeter data into hydrodynamical model: a global model and a regional model around Japan, J. of Oceanography, 56, 567-581.

W. H. Munk, D. E. Cartwright Philosophical Transactions of the Royal Society of London. Series A, Mathematical and Physical Sciences, Vol. 259, No. 1105 (May 19, 1966), pp. 533-5

Ray, R., 1999: A Global Ocean Tide model from Topex/Poseidon Altimetry, GOT99.2. Rapport n° NASA/TM-1999-209478, édité par Goddard Space Flight Center, NASA, Greenbelt, MD, USA. pp. 58.

Ray, R. (2008) GOT4.7, personnel communication

Savcenko, R. and W.Bosch (2004): Shallow water tide analysis with complementary tracks of Jason-1 and T/PEM.EGU General Assembly, Nice, France, April 25-30

Schrama E.J.O., R.D. Ray, A preliminary tidal analysis of Topex/Poseidon Altimetry, JGR Vol 99 No C12 pp 24799-24808, 1994. [pdf] [A8]

Schrama E., R. Scharroo, and M. Naeije, 2000, Radar Altimeter Database System (RADS): Towards a generic multi-satellite altimeter database system, USP-2 report 00-11, CRS/SRON, Delft, The Netherlands

Scharroo, R. and P. N. A. M. Visser, 1998, Precise orbit determination and gravity field improvement for the ERS satellites. J. Geophys. Res., 103, C4, 8113-8127

Smith A.J.E.,1999, Application of satellite altimetry for global ocean tide modelling. PhD. Delft Institute for Earth-Oriented Space Research. Delft University of technology. Faculty of Aerospace Engineering.

Smith, A. J. E., B. A. C. Ambrosius and K.F. Wakker(2000) Ocean tides from T/P, ERS-1 and GEOSAT altimetry. J. Geodesy 74:399-413

Smithson, M.J. 1992. Pelagic tidal constants – 3. IAPSO Publications Scientifique No. 35. Published by the International Association for the Physical Sciences of the Ocean (IAPSO) of the International Union of Geodesy and Geophysics. 191pp

Tierney, C.C., M.E. Parke and G.H. Born, 1998, An investigation of ocean tide derived from along-track altimetry, J. Geophys. Res. 103(C5) 10.723-10.287.

Wünsch, J., Schwintzer, P., Petrovic, S. (2005): Comparison of two different ocean tide models especially with respect to the GRACE satellite mission, Scientific Technical Report STR05/08, GeoForschungsZentrum Potsdam

7 Acknowledgement

We gratefully acknowledge the provision of

- the FES2004 model by T. Lettellier,
- the revised version of FES2004 model by AVISO
- TPXO7.1 by Gary Egbert,
- GOT4.7 by Richard Ray,
- the DAC (MOG2D) correction and by CLS (LEGOS),
- the DEOS orbits for the ESA satellites, and of
- the ocean bottom pressure records from BODC.

This study has been funded by the Deutsche Forschungsgemeinschaft (DFG) under the grant BO 1228/6-1.

A Appendix

The following appendix provides maps showing the geographical distribution of amplitudes (always top panels) and phases (always bottom panels) for the estimated residuals of all constituents. Zoomed maps are provided for the Patagonian Shelf (A.1), the North-West European Shelf (A.2), and the Yellow Sea (A.3). Section A.4 provides global maps of the residuals.

The 7.5'x7.5' grids of the EOT08a model are available at the anonymous ftp

```
ftp.dgfi.badw.de
```

in directory

```
pub/EOT08a
```

together with the pdf version of this report. The tables are provided in NetCDF format, following the COARDS, version 1.0 standard. NetCDF (network Common Data Form) is a set of software libraries and machine-independent data formats that support the creation, access, and sharing of array-oriented scientific data (see http://www.unidata.ucar.edu/software/netcdf/ for details). The grids can also be read by the Generic Mapping Tools (GMT), open source software developed and maintained by Paul Wessel and Walter H. F. Smith (see http://gmt.soest.hawaii.edu/).

A.1 Patagonian Shelf

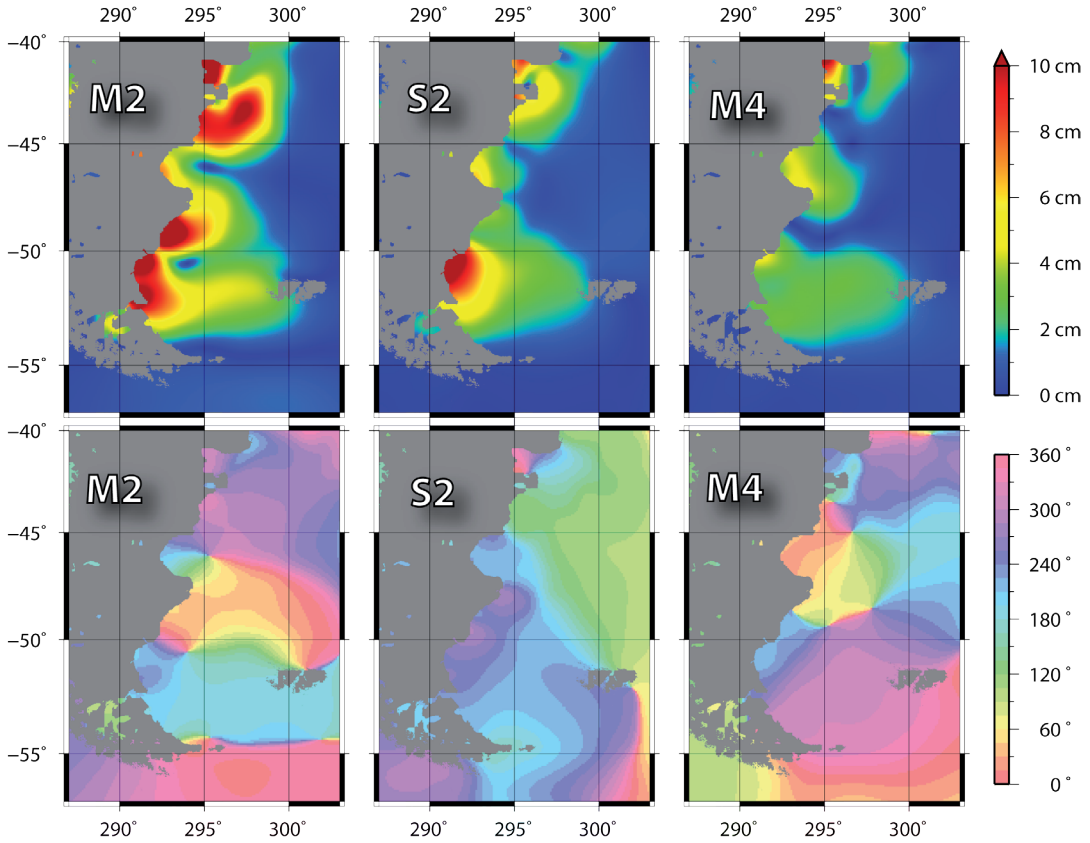

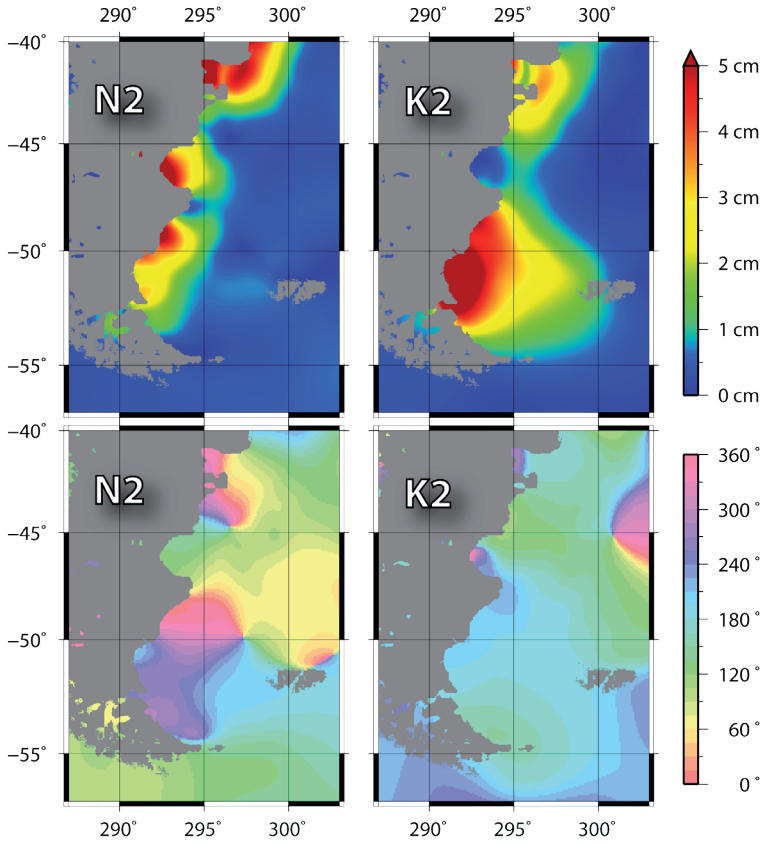

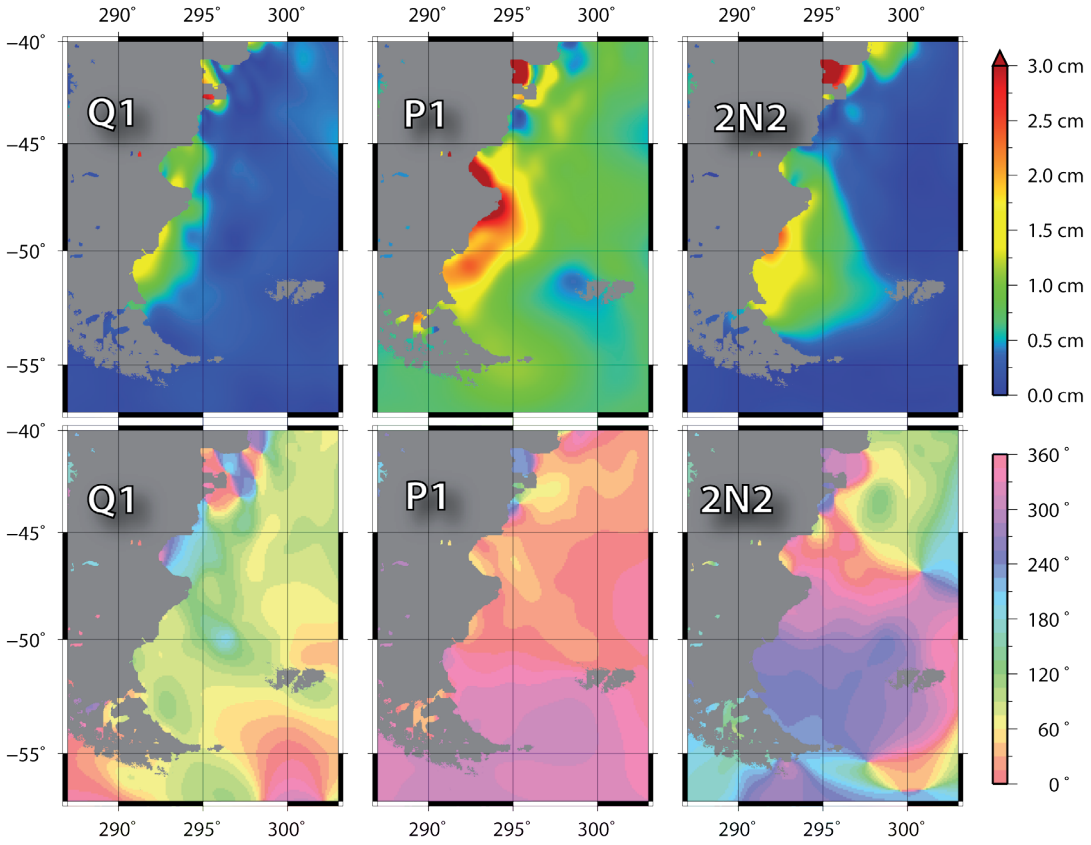
290° 295° 300°
−40°
−45°
−50°
−55°
Q1
P1
2N2
3.0 cm
2.5 cm
2.0 cm
1.5 cm
1.0 cm
0.5 cm
0.0 cm
360 °
300 °
240 °
180 °
120 °
60 °
0 °

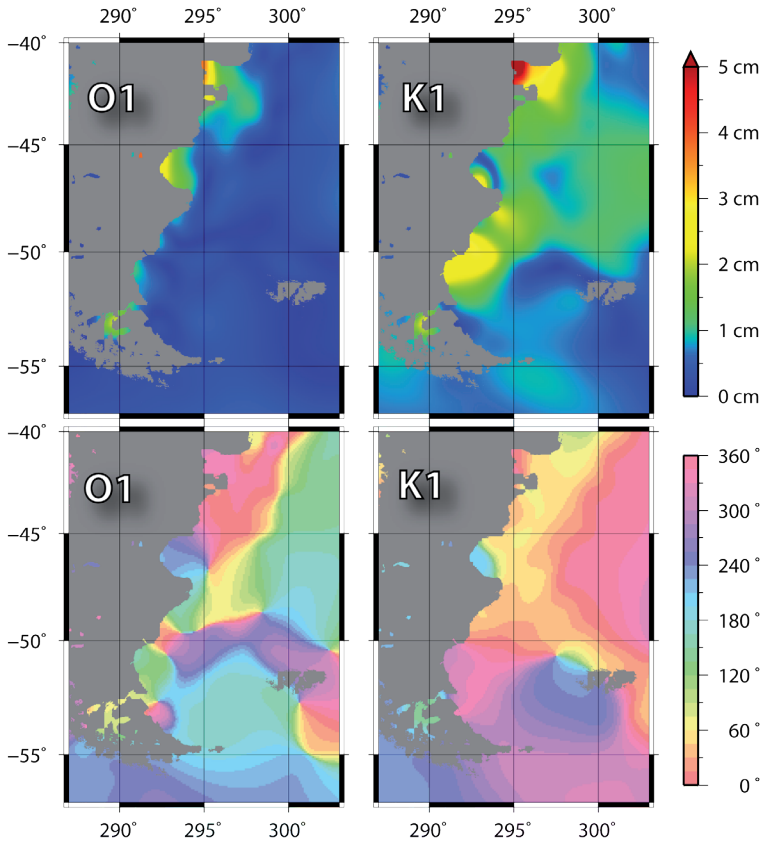
290° 295° 300°
−40°
−45°
−50°
−55°
O1
K1
5 cm
4 cm
3 cm
2 cm
1 cm
0 cm
360 °
300 °
240 °
180 °
120 °
60 °
0 °

A.2 North-West European Shelf

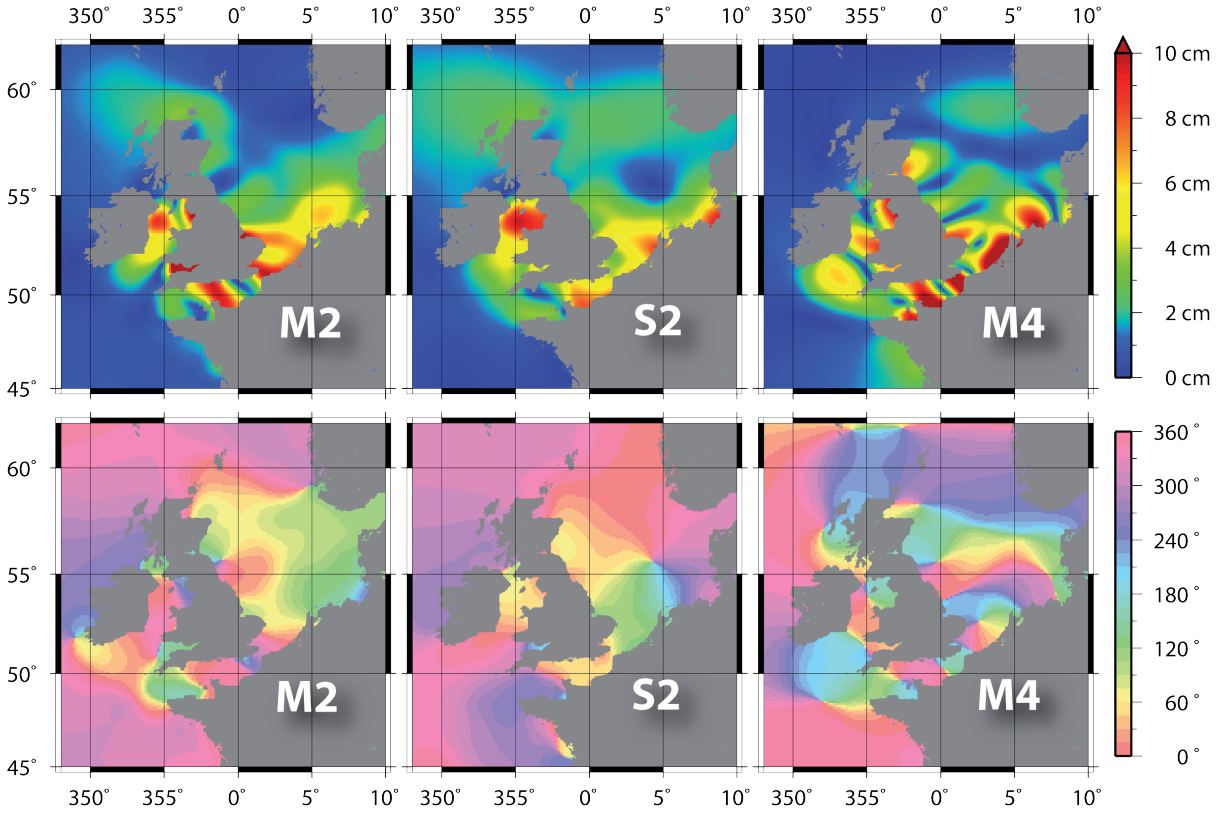

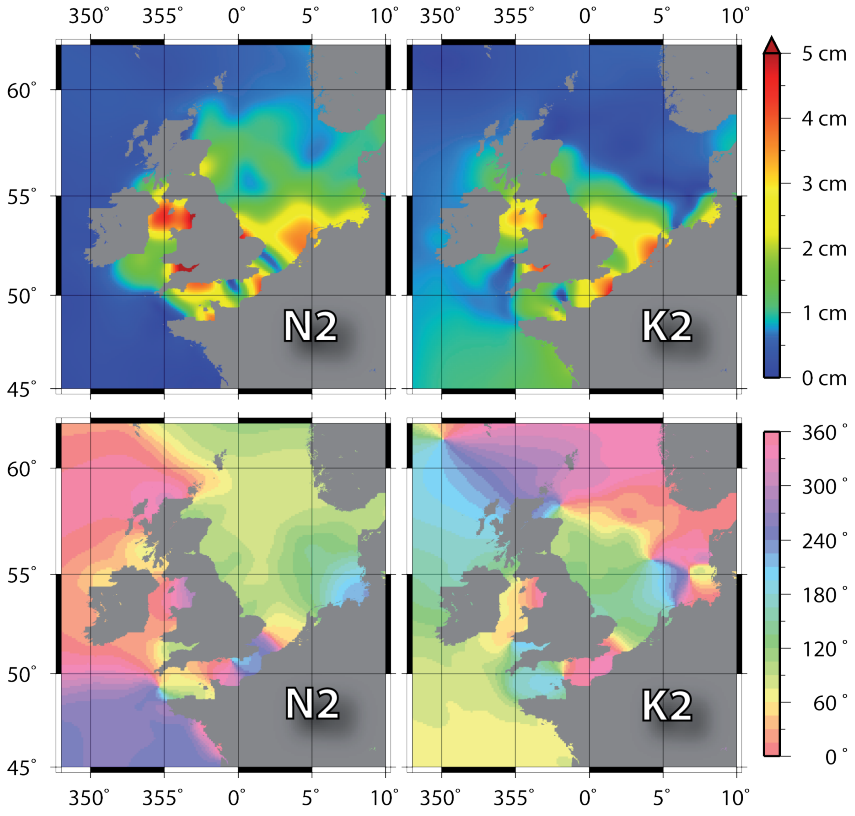

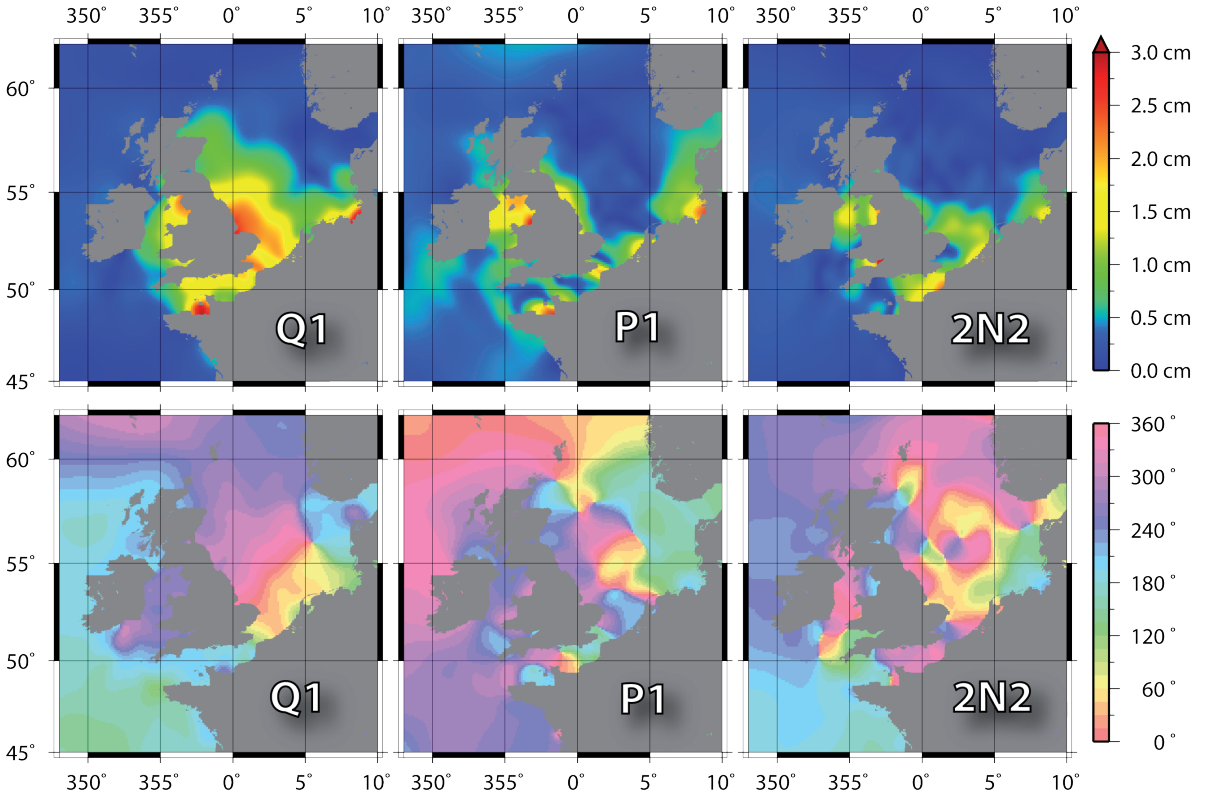
Q1
P1
2N2
3.0 cm
2.5 cm
2.0 cm
1.5 cm
1.0 cm
0.5 cm
0.0 cm
360 °
300 °
240 °
180 °
120 °
60 °
0 °

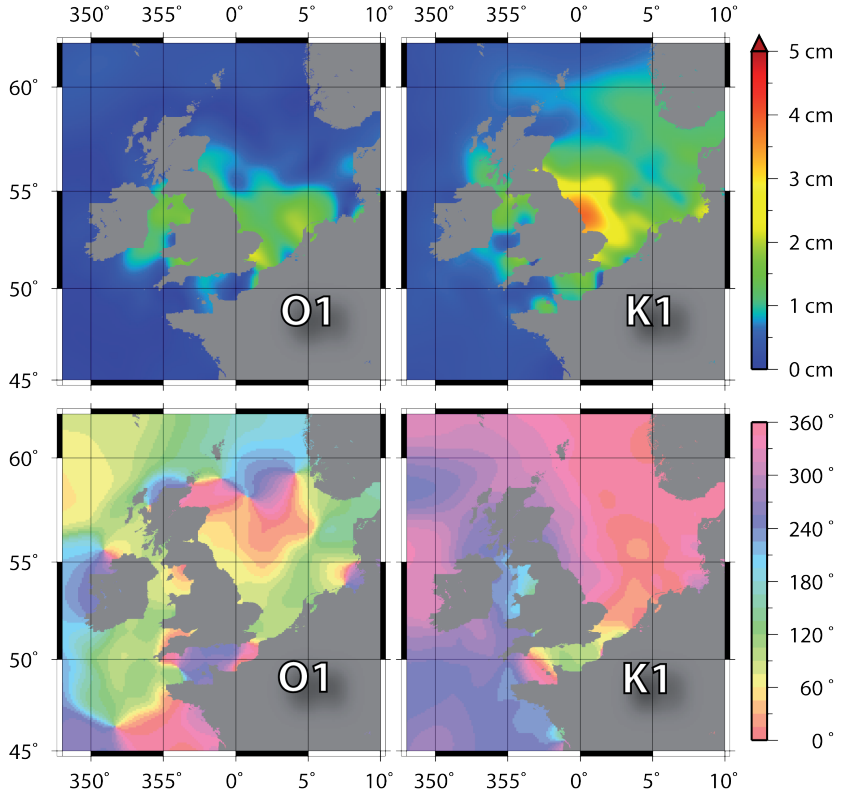
O1
K1
5 cm
4 cm
3 cm
2 cm
1 cm
0 cm
360 °
300 °
240 °
180 °
120 °
60 °
0 °

A.3 Yellow Sea

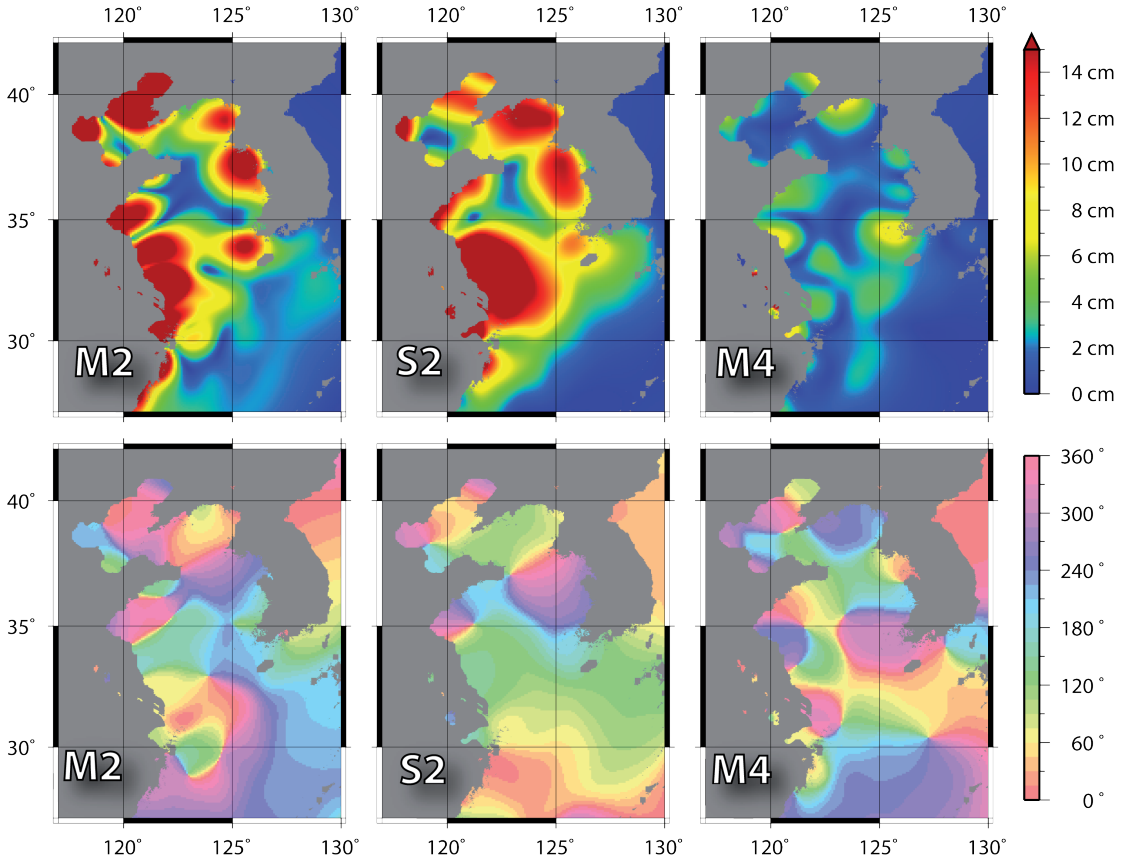

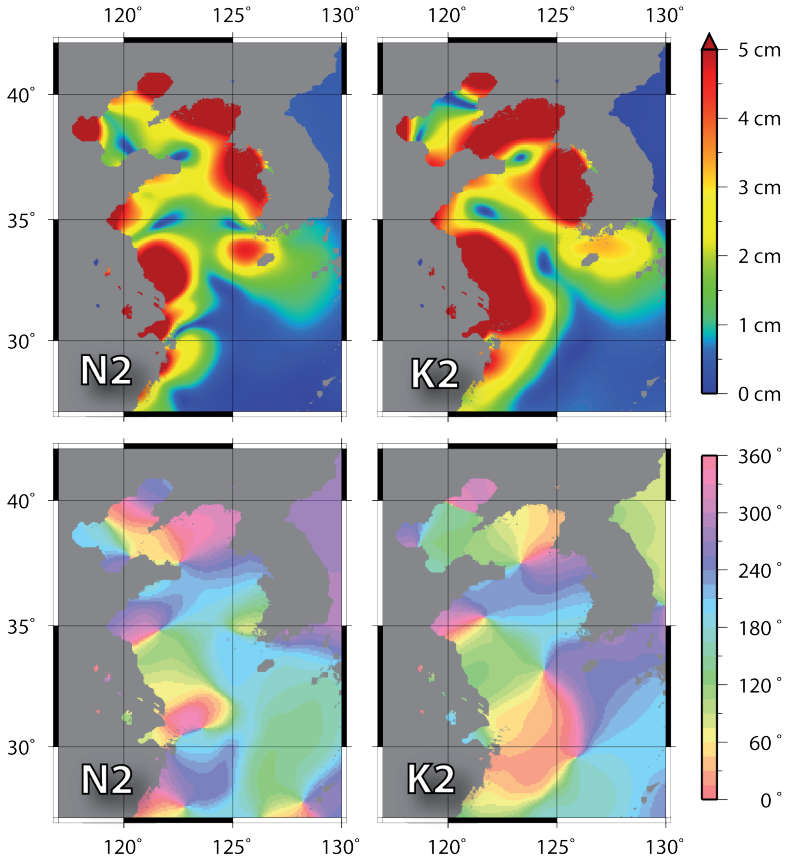

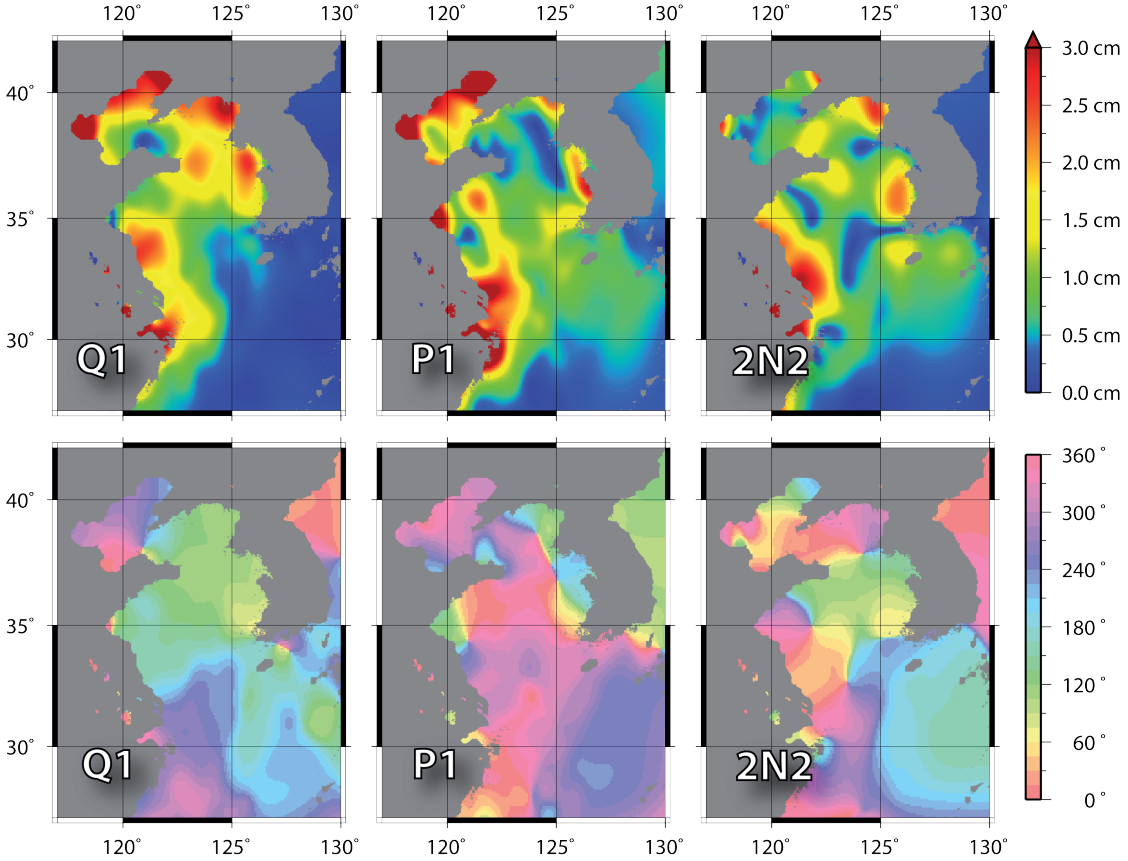
120° 125° 130°
40° 35° 30°
Q1
P1
2N2
3.0 cm
2.5 cm
2.0 cm
1.5 cm
1.0 cm
0.5 cm
0.0 cm
360 °
300 °
240 °
180 °
120 °
60 °
0 °

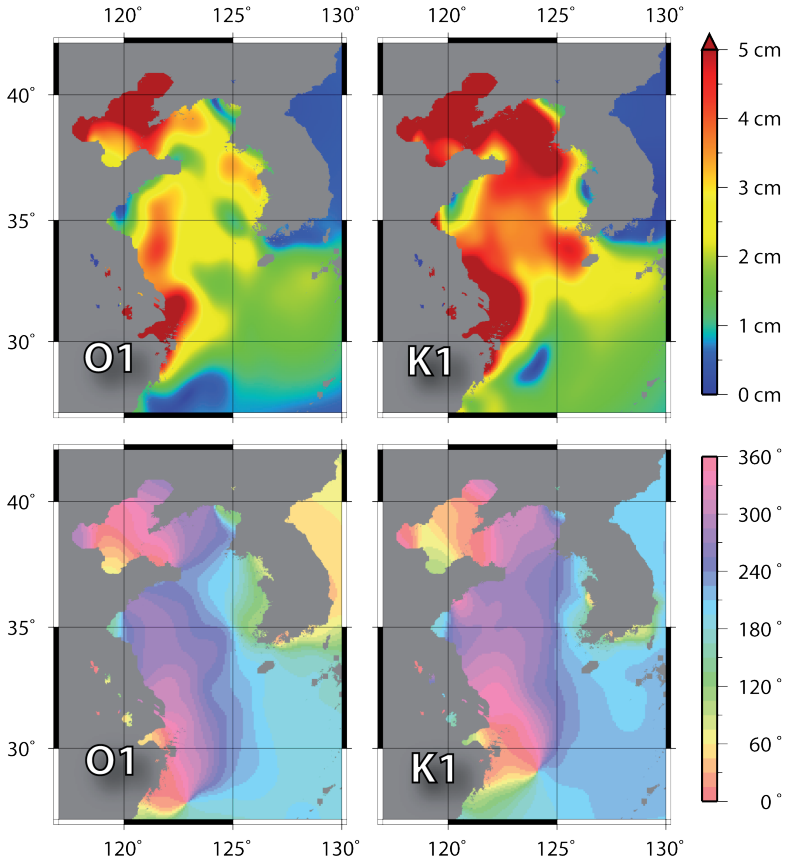
120° 125° 130°
40° 35° 30°
O1
K1
5 cm
4 cm
3 cm
2 cm
1 cm
0 cm
360 °
300 °
240 °
180 °
120 °
60 °
0 °

A.4 Global Maps

M2 residual tidal constituent

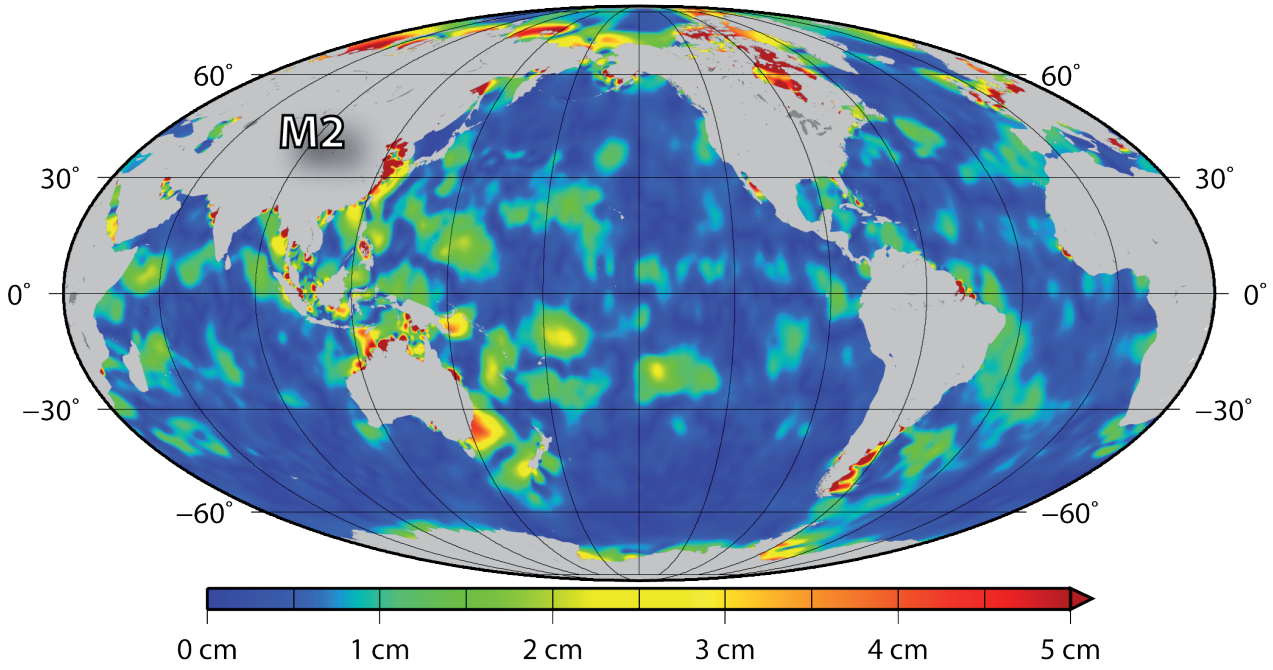

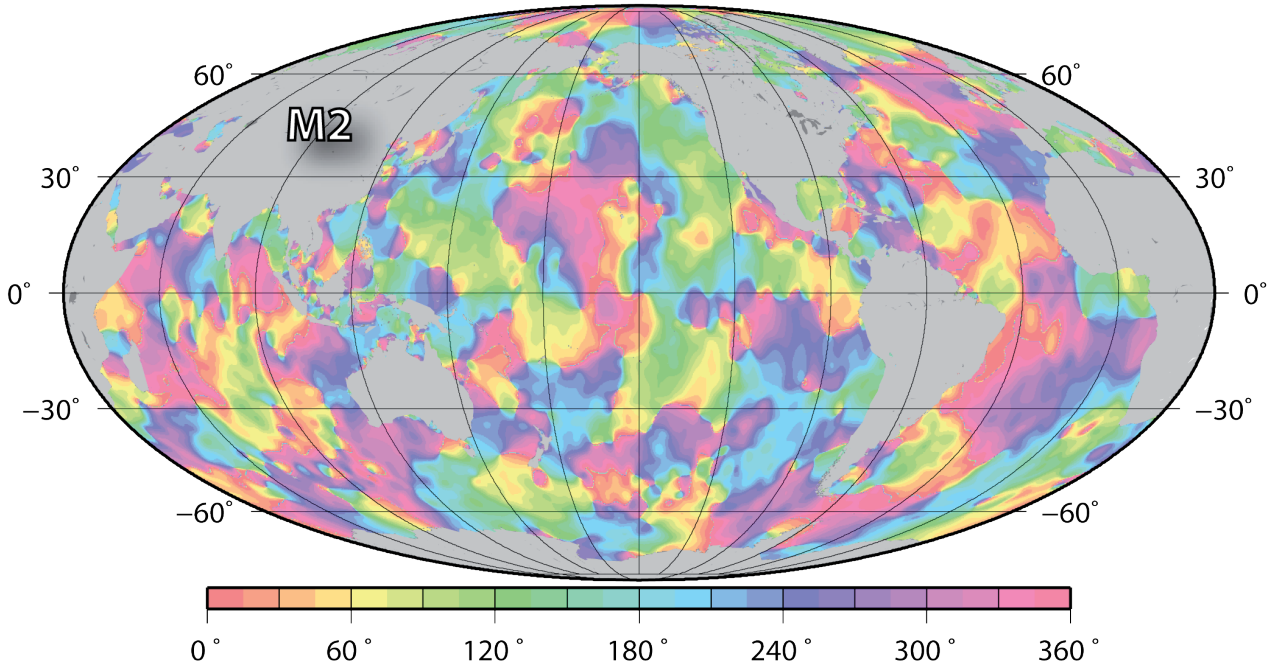

N2 residual tidal constituent

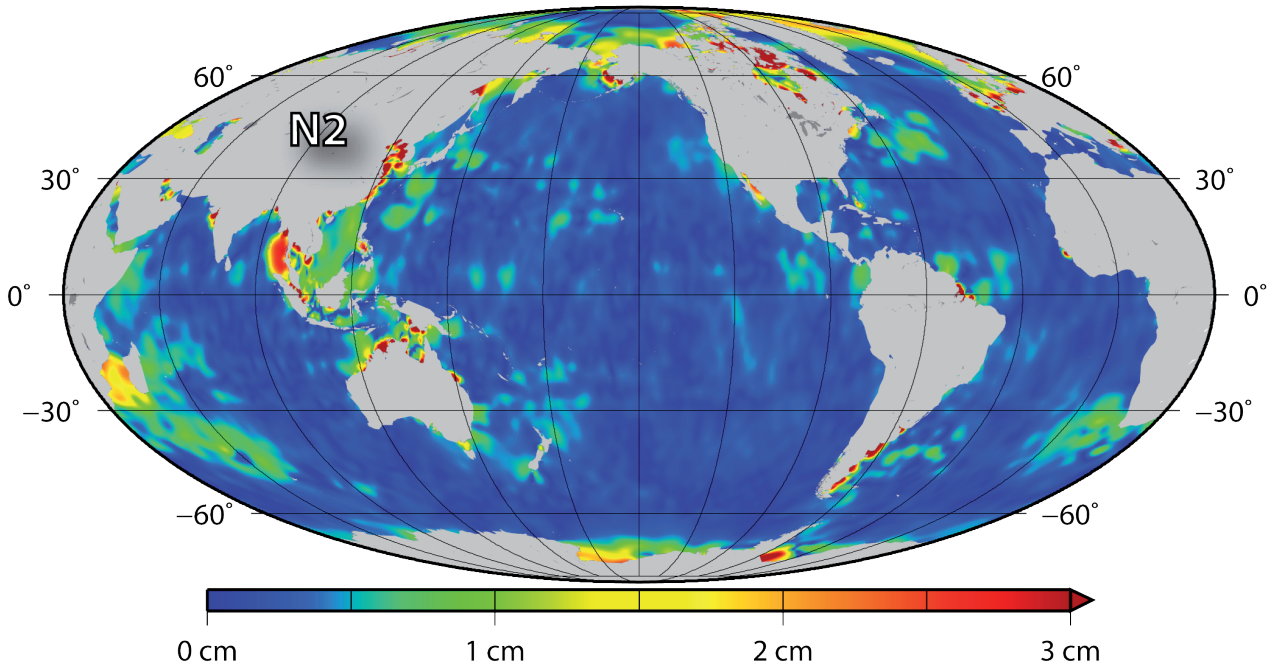

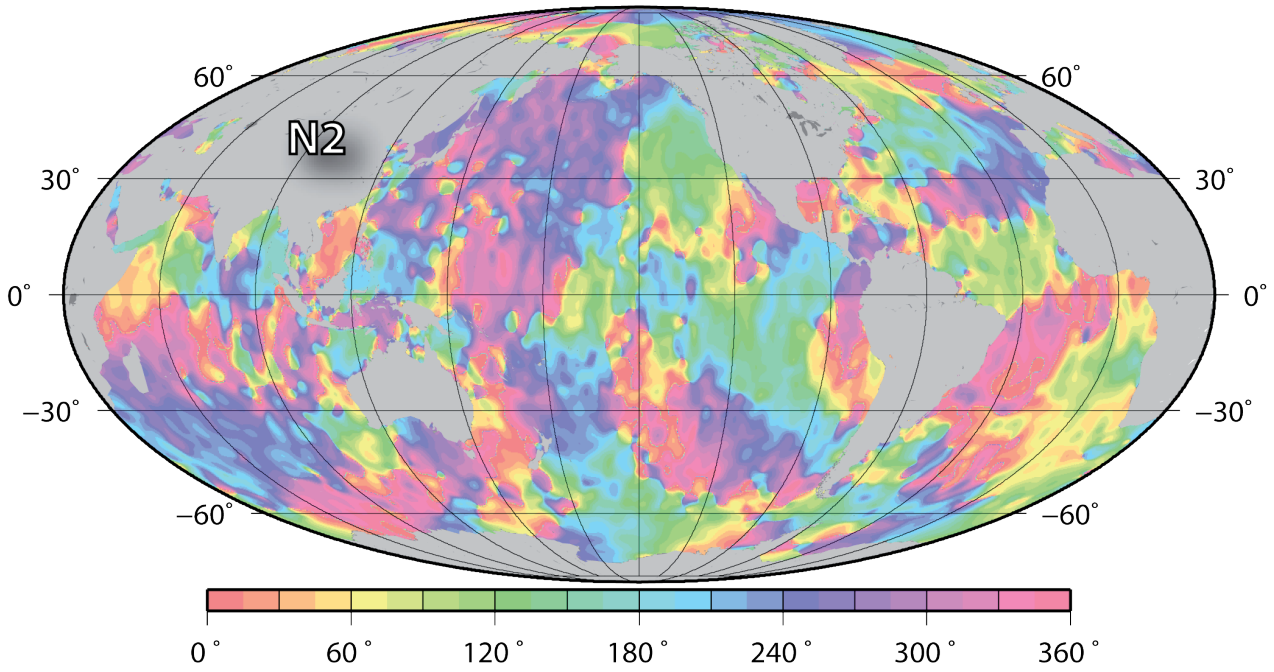

K2 residual tidal constituent

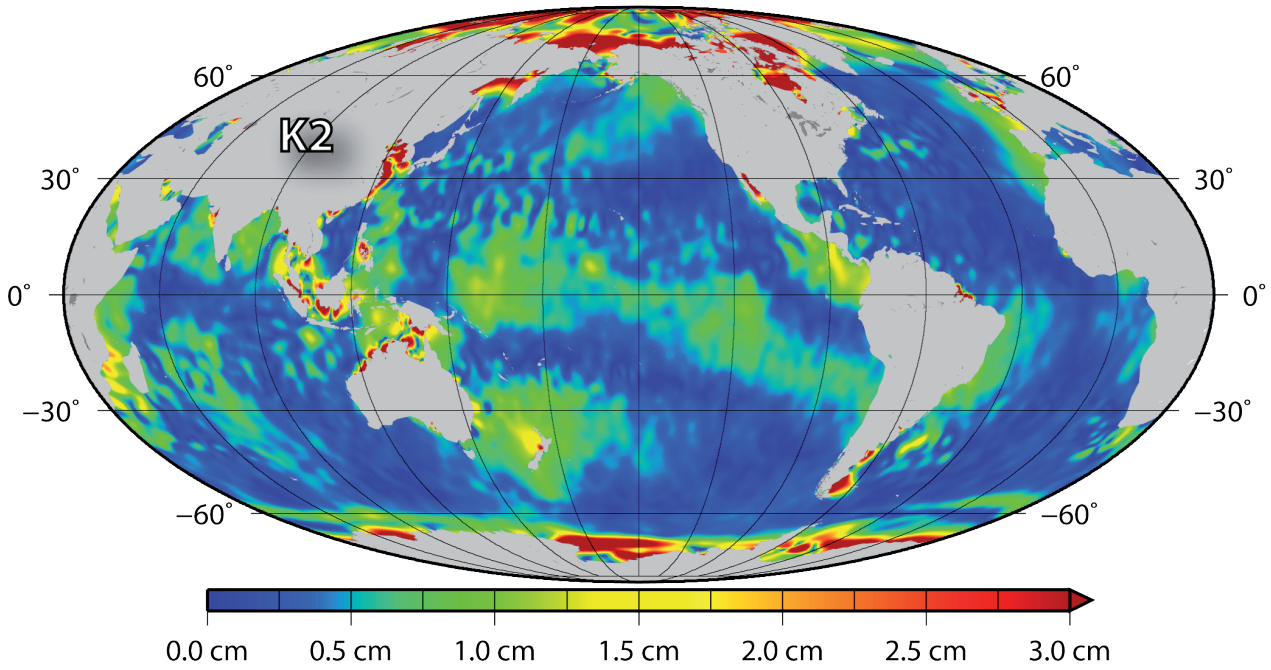

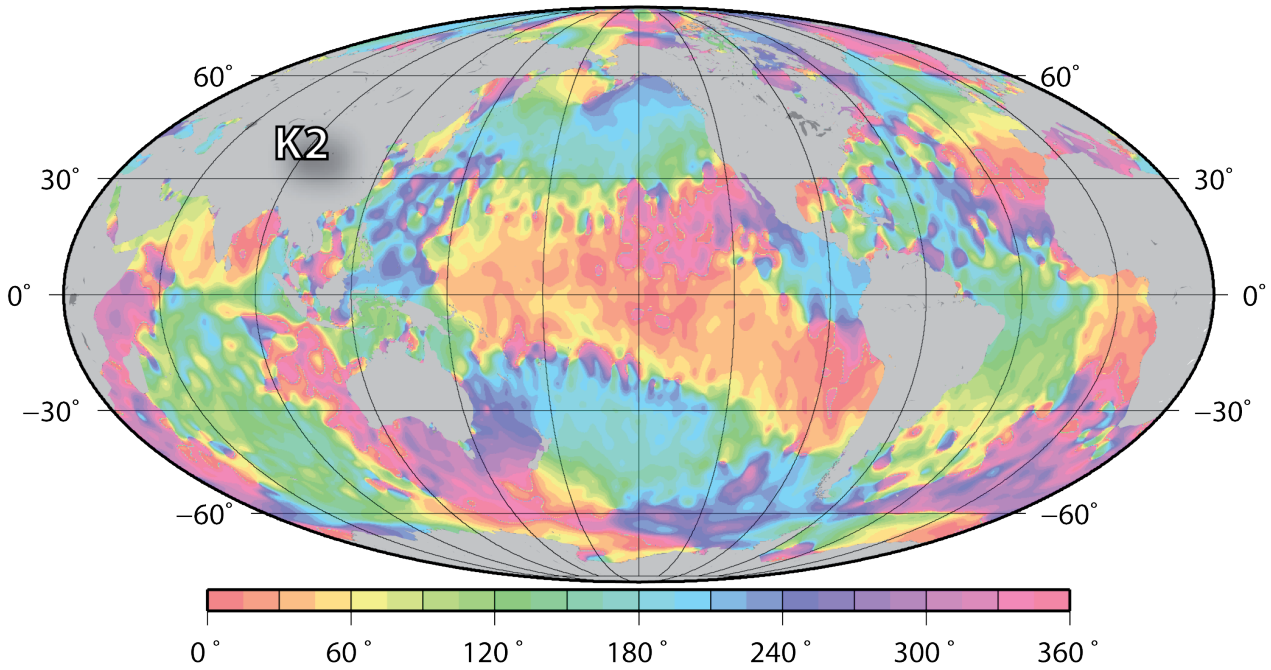

S2 residual tidal constituent

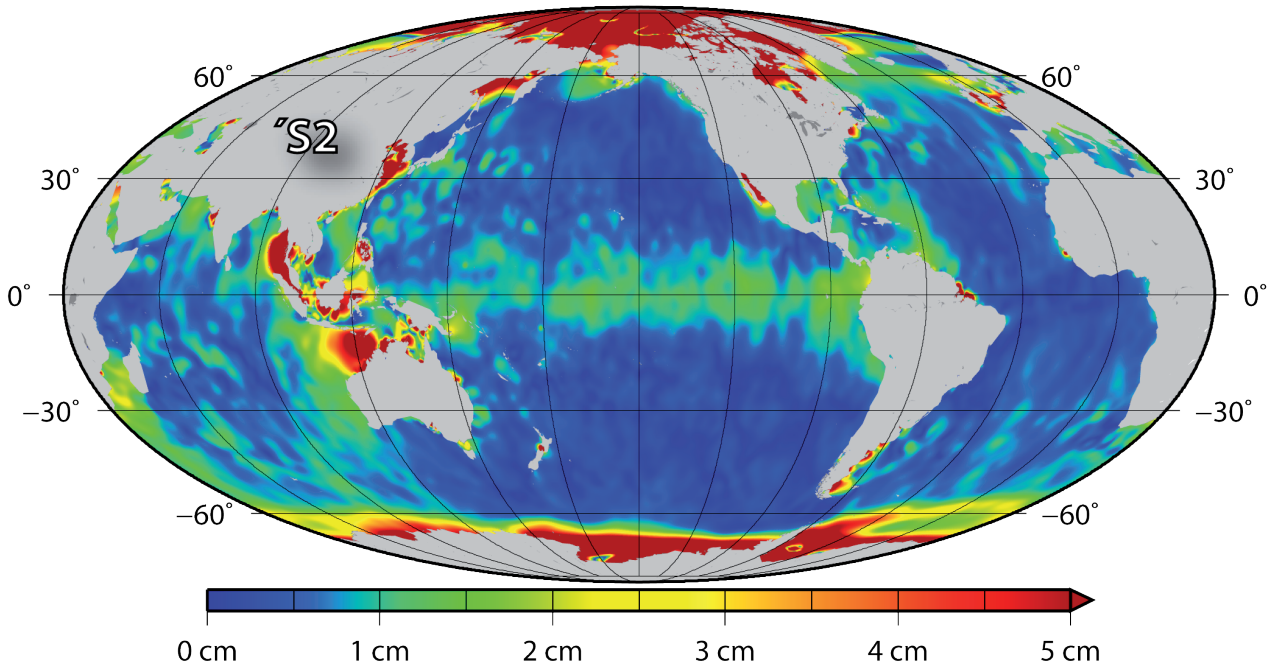

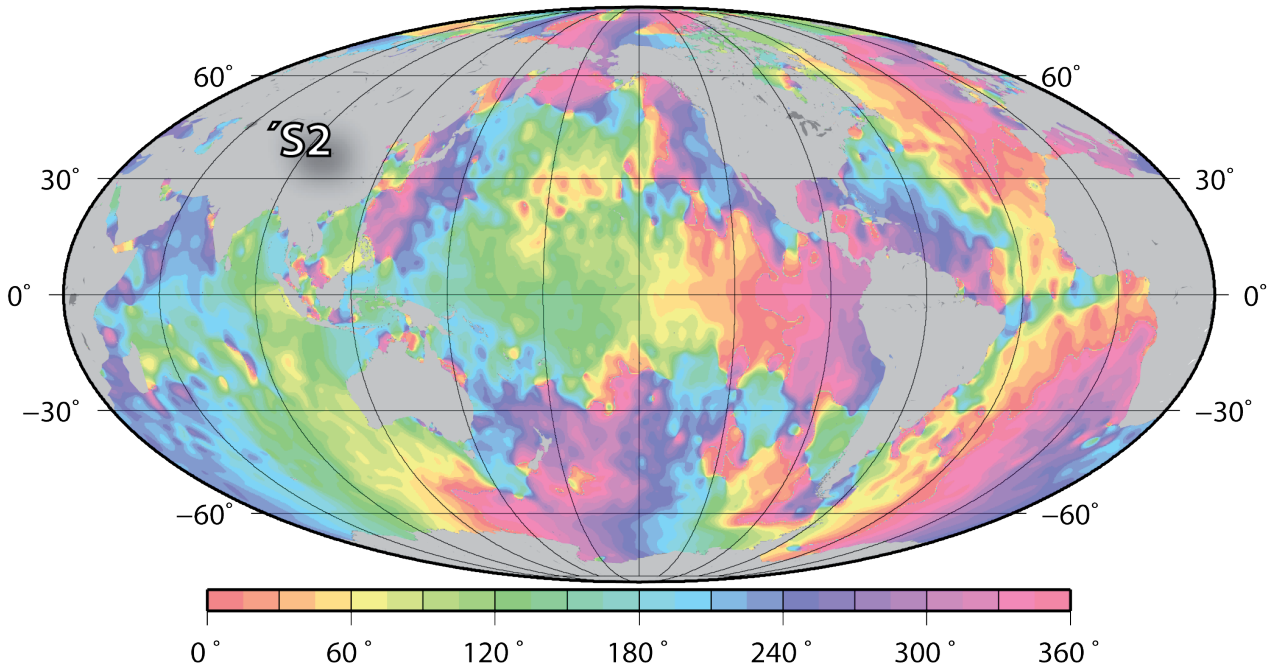

K1 residual tidal constituent

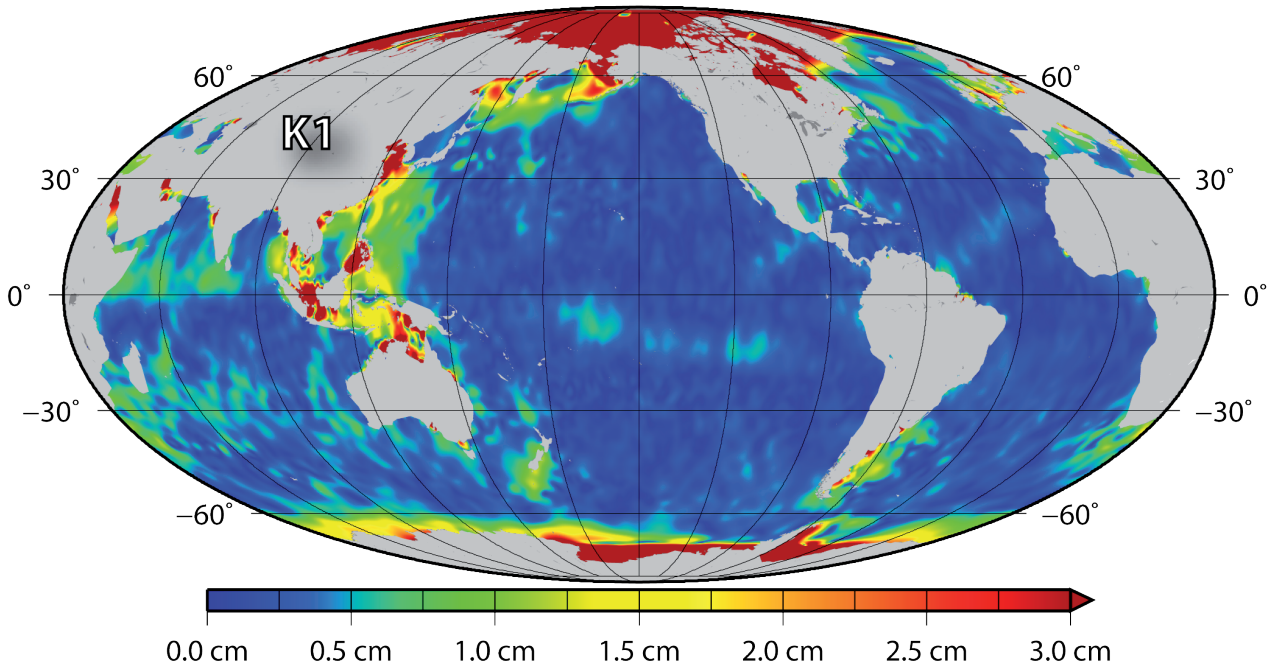

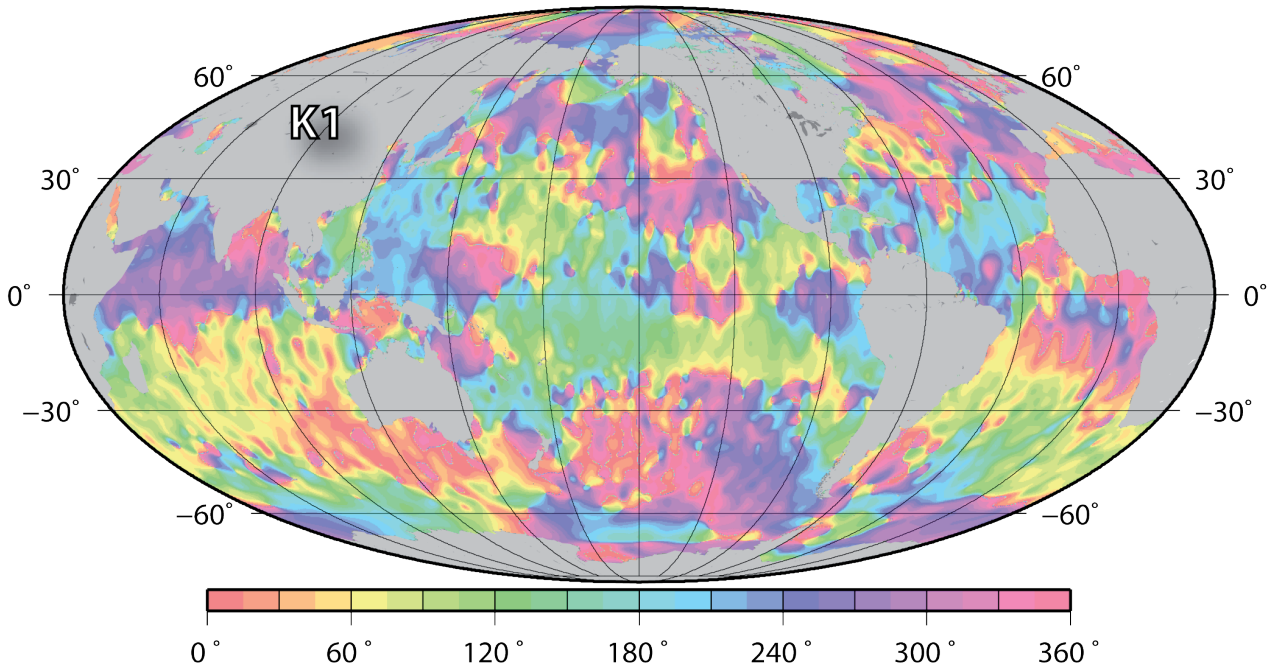

O1 residual tidal constituent

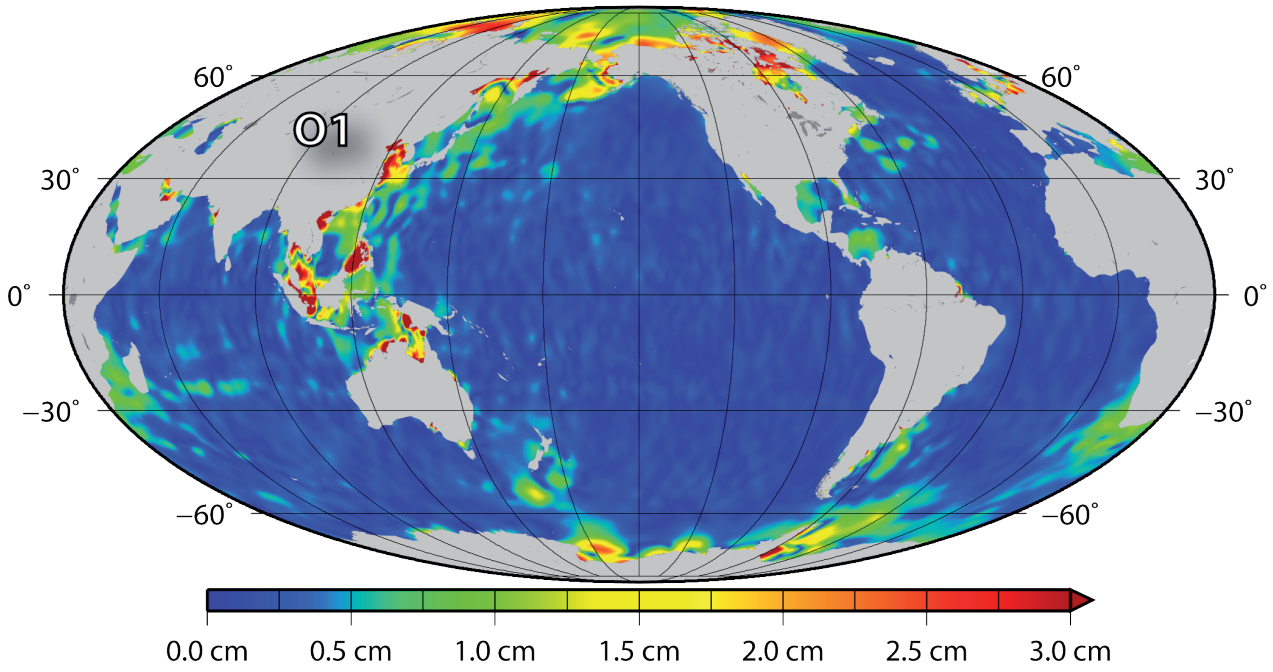

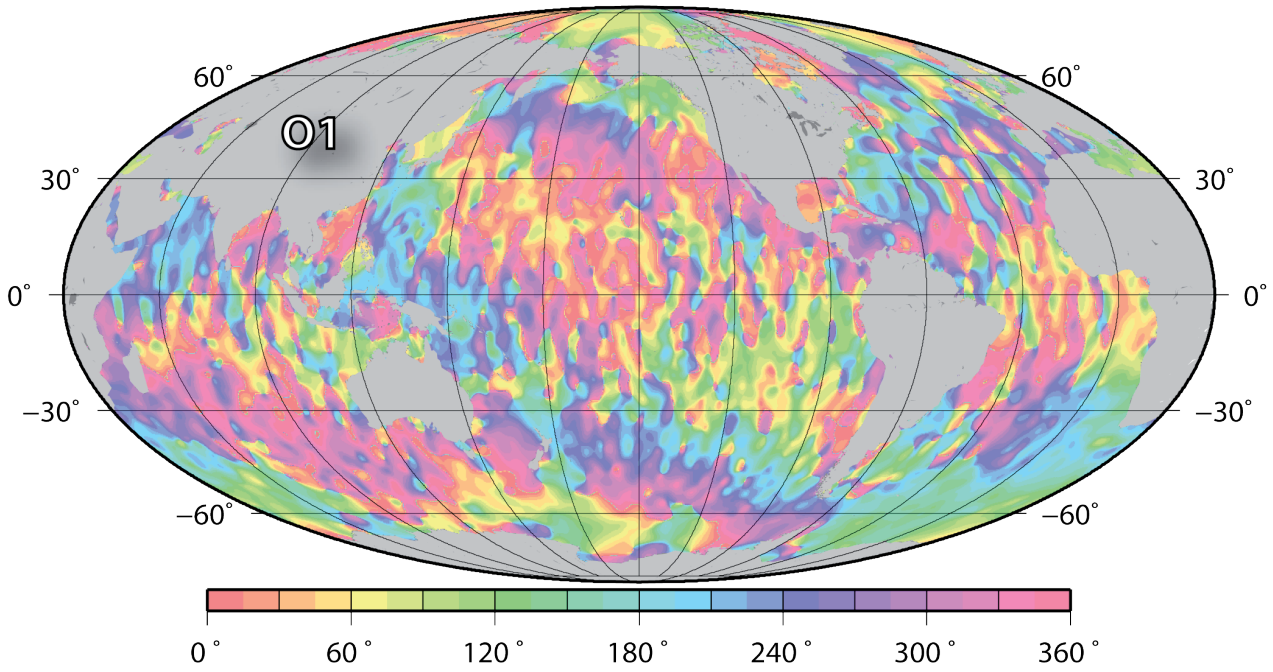

P1 residual tidal constituent

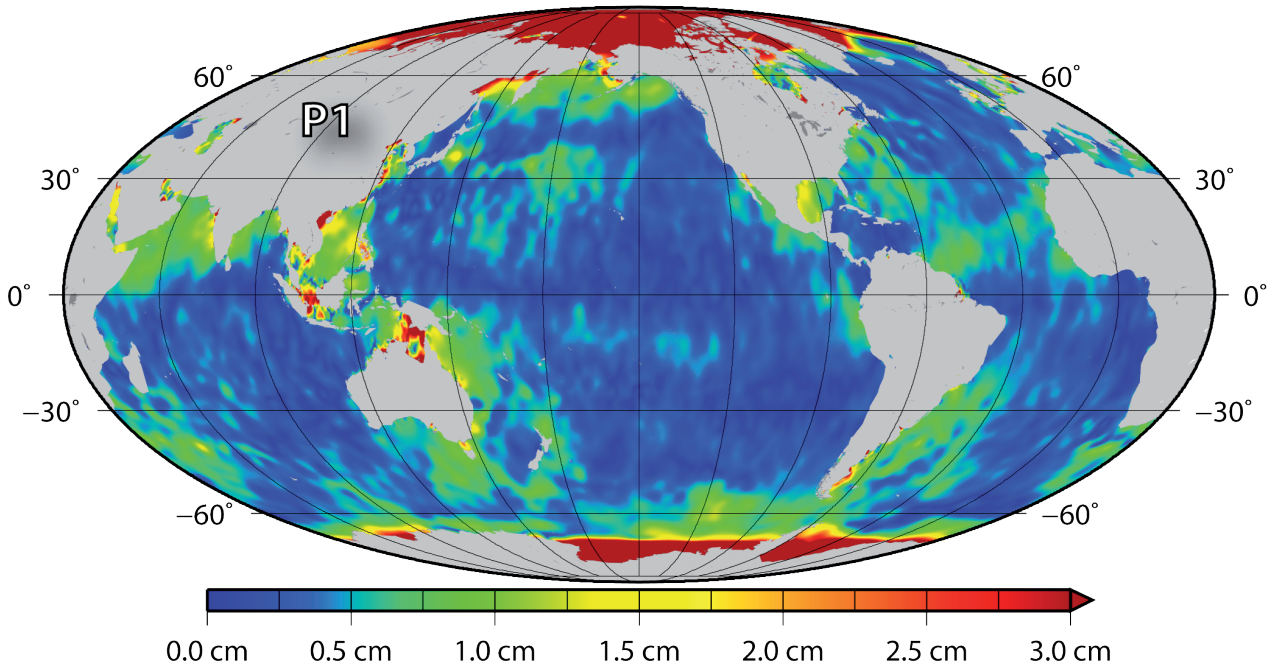

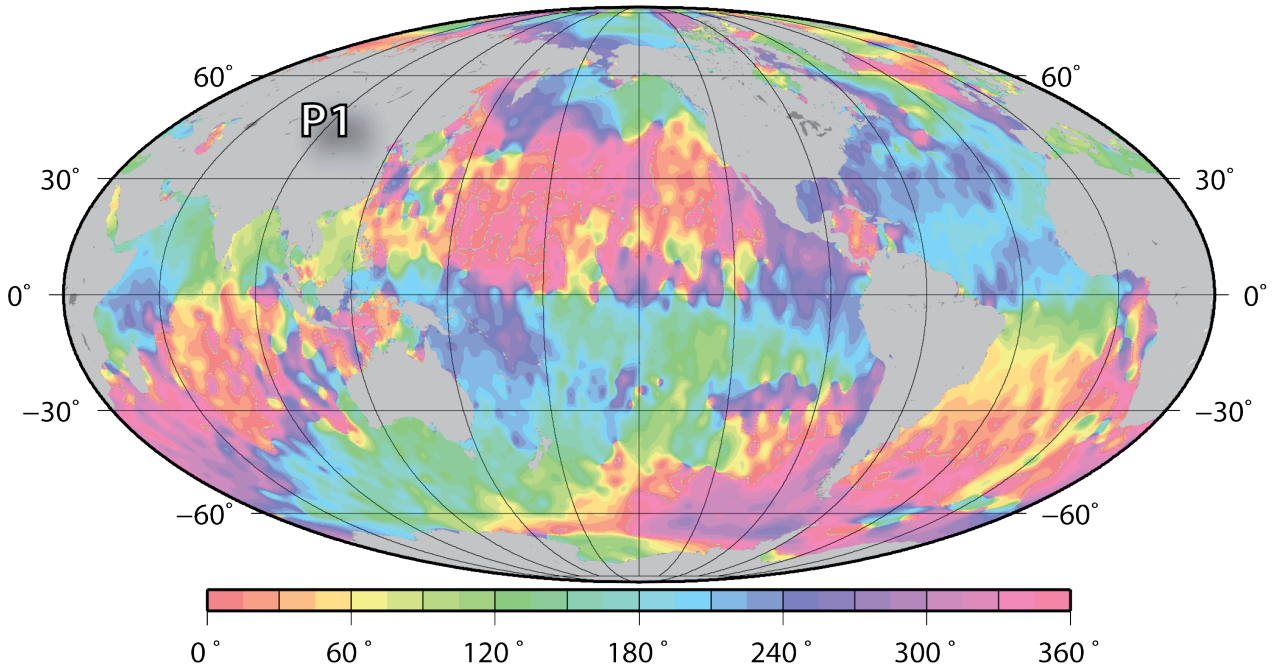

Q1 residual tidal constituent

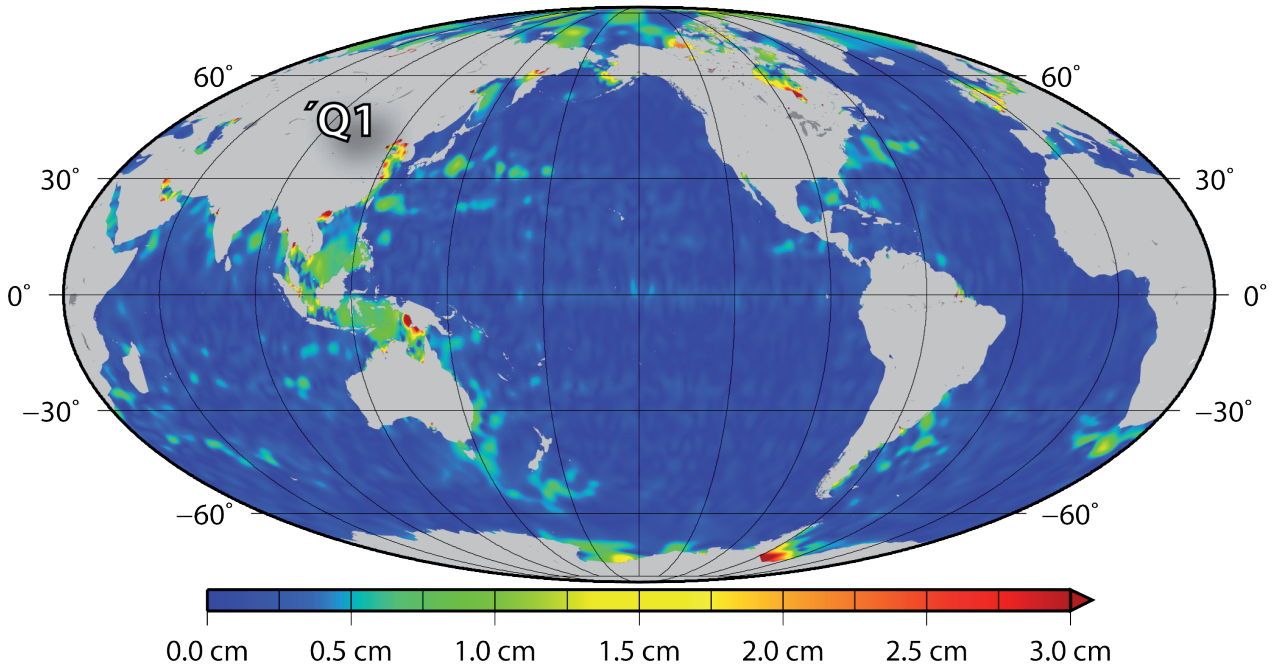

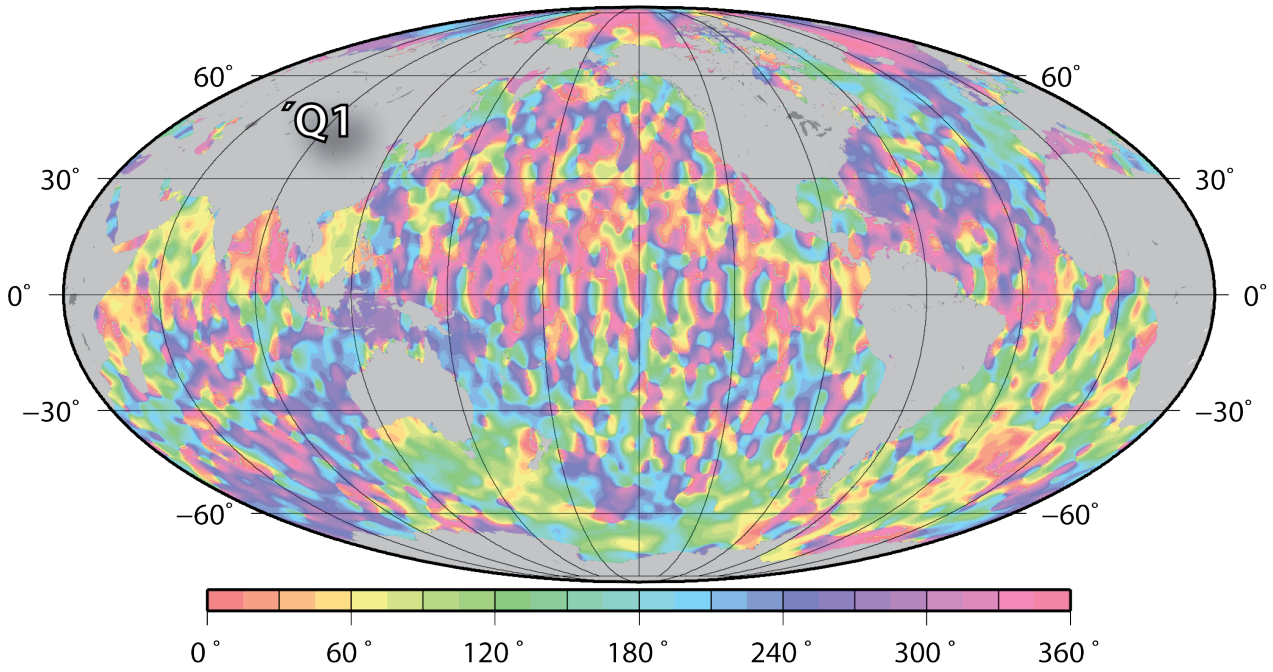

2N2 residual tidal constituent